A Review of Crop Height Retrieval Using InSAR Strategies: Techniques and Challenges

Noelia Romero-Puig, *Student Member, IEEE*, Juan M. Lopez-Sanchez, *Senior Member, IEEE*

***Abstract*—This work compares the performance of four different interferometric synthetic aperture radar techniques for the estimation of rice crop height by means of bistatic TanDEM-X data. Methods based on the interferometric phase alone, on the coherence amplitude alone, on the complex coherence value, and on polarimetric interferometry (PolInSAR) are analyzed. Validation is conducted with reference data acquired over rice fields in Spain during the Science Phase of the TanDEM-X mission. Single- and dual-polarized data are exploited to provide also further insights into the polarization influence on these approaches. Vegetation height estimates from methodologies based on the interferometric phase show a general underestimation for the HH channel (with a bias that reaches around 25 cm in mid July for some fields), whereas the VV channel is strongly influenced by noisy phases, especially at large incidences (RMSE = 31 cm). Results show that these approaches perform better at shallower incidences than the methodologies based on coherence amplitude and on PolInSAR, which obtain the most suitable results at steep incidences, with RMSE values of 17 and 23 cm. On the contrary, at shallower incidences, they are highly affected by very low input coherence levels. Hence, they tend to overestimate vegetation height.**

***Index terms*—** Bistatic radar, height, InSAR, PolInSAR, rice, TanDEM-X.

I. Introduction

VEGETATION height is a key feature in crop and forest monitoring from which other important variables, such as yield and biomass, can be retrieved. Therefore, a systematic acquisition of quantitative information about vegetation height from remote sensing data is of major relevance to support agricultural and forest management services. The exploitation of vegetation height information in the agricultural domain presents diverse objectives. For instance, during the vegetative stage of cereals, the growth rate is a clear indicator of the right development of the crops which serves to detect anomalies and cultivation problems. Then, crop height during the reproductive and maturation stages is frequently associated with total biomass, which in turn is related to the final yield. Among all remote sensing techniques, synthetic aperture radar (SAR) provides a reliable observation scheme thanks to its all-weather day-and-night imaging capability. SAR offers different types of data which can be exploited as inputs for vegetation height retrieval. Most techniques are based on intensity data (i.e. backscattering coefficient), polarimetry and/or interferometry. A comparison of different SAR-based approaches for the retrieval of crop height was recently published in [1].

Interferometric SAR (InSAR) approaches are based on the exploitation of the correlation (i.e. coherence) and phase difference between two SAR acquisitions [2]. Notably, these two magnitudes are dependent on the vertical distribution of elements in the scene, hence providing an explicit sensitivity to vegetation height [3]. However, a successful crop height retrieval from data acquired by airborne or spaceborne sensors is bound to a short temporal separation between the SAR acquisitions [4], [5]. Otherwise, temporal decorrelation affects the interferometric products and the results are not valid. In this regard, conventional repeat-pass systems based on SAR satellites are of limited use for InSAR-based crop height estimation due to the rapid growth of crops and to the movement of the plants associated with wind. This situation changed with the launch of the TanDEM-X system [6], a two-satellite flying formation characterized by single-pass acquisitions, i.e. two images acquired simultaneously, hence in absence of temporal decorrelation. In addition, during the Science Phase of the TanDEM-X mission, from April to September 2015, large spatial baselines (2–3 km) were available, which provided, for the first time, the sensitivity requirements for the estimation of agricultural crop variables from space-based single-pass InSAR data [7]. To date, several studies have demonstrated the potential of the TanDEM-X sensor in retrieving vegetation height in crop scenarios through a variety of InSAR techniques [1], [8]–[12].

This work is aimed at comparing all available InSAR techniques for crop height estimation based on the exploitation of TanDEM-X data. On the basis that the interferometric phase is proportional to the height of the scattering phase center, Rossi and Erten reported successful results in measuring crop height by using only the interferometric phase as input feature [8]. Later on, single-polarization InSAR data were employed to retrieve forest height using only the coherence amplitude [13]–[16]. However, this approach has not been applied to crops yet. In another study, the complex interferometric coherence (i.e. both amplitude and phase) was employed by Lee *et al.* to estimate rice height [12]. Finally, polarimetric SAR interferometry (PolInSAR), which combines polarimetric and interferometric information, has been also tested in agricultural scenarios in [1], [9]. It is important to note that in the comparison of methods published in [1] the approaches based on the coherence amplitude and on the complex coherence were not considered. Therefore, this work is aimed at filling this gap and comparing all the known InSAR-based approaches.

This work was supported by the Spanish Ministry of Science and Innovation, the State Agency of Research (AEI) and the European Funds for Regional Development (EFRD) under Project TEC2017-85244-C2-1-P. Noelia Romero received a grant from the Generalitat Valenciana and the European Social Fund (ESF) [ACIF/2018/204].

All authors are with the Institute for Computer Research (IUII), University of Alicante, P.O.Box 99, E-03080 Alicante, Spain (e-mail: noelia.romero@ua.es, juanma-lopez@ieee.org).

For this purpose, dual-pol TanDEM-X data acquired during the Science Phase are used. Previous works have revealed the polarization dependence of the penetration capability of the SAR signal [8], [17]. Therefore, the separate study of both polarization channels available in the dual-pol data set, i.e. HH and VV, is relevant to shed some light into the extent of the polarization influence on crop monitoring. Moreover, the interest of using each polarization channel separately relies on the fact that the standard acquisition mode of TanDEM-X is single-pol [6], which presents a much wider coverage and better azimuth resolution than dual-pol. Furthermore, the influence of incidence angle and baseline on the performance of these techniques is analyzed in order to assess the accuracy and robustness under different conditions.

The structure of this paper is as follows. Section II presents the test site and the TanDEM-X data set employed. The InSAR methodologies under study, including the common processing prior to the inversion, are described in Section III. In Section IV, the results from all inversion methodologies are compared and discussed. In the end, the conclusions are drawn in Section V.

II. Test site and Data set

A. Test site and ground campaign data

A paddy rice area in Spain is selected for the assessment of rice crop height retrieval (see Fig. 1). The test site covers an area of 30 km $\times$ 30 km around the mouth of the Guadalquivir river, Sevilla, SW of Spain (37.1 N, 6.15 W). As opposed to other cultivation practices [8], [12], the parcels are kept flooded during the whole rice growth cycle (from May to October), and not only in the early vegetative stage.

During a campaign in 2015, the local association of rice farmers gathered some agricultural descriptors of four rice fields on a weekly basis. The specific location of these fields is shown in the right part of Fig. 1. The four fields are characterized by the same rice species, which corresponds to *Oriza sativa L.* This species is the dominant monoculture in the Guadalquivir marshes, with a stable area of around 37,000 ha over the last twenty years. Among the different rice varieties, the one of the monitored fields is an *Indica* long grain type named *puntal*, which represents more than 50% of rice paddies in the last ten years in the Sevilla province [18]. Phenological information according to the BBCH (*Biologische Bundesanstalt, Bundessortenamt und CHemische Industrie*) [19] scale and above-water vegetation height are available. This study area has been widely evaluated for rice crop monitoring in previous studies, e.g. [9], [20]–[24].

B. TanDEM-X data and InSAR processing

In the present study, we have exploited dual-pol TanDEM-X SAR data acquired during the Science Phase of this mission. The acquisition period covered most of the phenological cycle of the monitored rice crops, from May to early September in 2015. The TanDEM-X data acquired during this phase was especially chosen due to its large spatial baseline (2–3 km) and short height of ambiguity (HoA), e.g. 2.5 m for 22.7 degrees of incidence angle. This is a key parameter (described in Section III) in determining the sensitivity of the interferometric system, which was for the first time suitable for crop monitoring. Moreover, the advantage of using dual-pol images is that they allow us to compare vegetation height estimates obtained from single-pol approaches using the two different polarimetric channels, i.e. HH and VV. The main characteristics of these images are summarized in Table I.

TABLE I
TanDEM-X system parameters and acquisition dates of the data sets over Sevilla test site

Incidence angle	HoA [m]	κ_Z [rad/m]	Date range	Day of Year (DoY)
22.7 deg.	2.53	2.48	2015.06.04–08.31	155–243
30 deg.	3.49	1.80	2015.05.04–09.02	124–245
39 deg.	5.81	1.08	2015.05.30–08.26	150–238

The data sets were gathered with three different incidence angles, which correspond to three different relative orbits. It is worth mentioning that the vertical wavenumber (κ_Z) and HoA are expressed in absolute value in Table I. However, depending on the relative position of the master and slave images at the moment of acquisition, their sign can be either positive or negative. This needs to be accounted for in the InSAR inversion methodologies.

Each TanDEM-X product contains a pair of dual-pol images acquired at HH and VV polarization channels [6]. Each dual-pol acquisition is expressed as a scattering vector $\vec{k}_1 = [S^1_{\text{HH}} S^1_{\text{VV}}]^T$ and $\vec{k}_2 = [S^2_{\text{HH}} S^2_{\text{VV}}]^T$, where S^n_{PP} represents the complex scattering amplitude at the n-th end of the spatial baseline. The effective spatial baseline, i.e. physical separation between satellites, drives the vertical wavenumber κ_Z [25], [26] as follows:

$$\kappa_Z = m \frac{2\pi B_\perp}{\lambda R \sin\theta_0}, \tag{1}$$

where $B_\perp$ is the perpendicular baseline, λ is the wavelength, R is the slant-range distance, and θ_0 is the incidence angle. Parameter m accounts for the acquisition mode: $m = 2$ for monostatic acquisitions, and $m = 1$ for bistatic acquisitions [27]. From equation (1), the maximum height that can be unambiguously estimated is defined as HoA $= {}^{2\pi}/_{\kappa_Z}$. The smaller the HoA, the higher sensitivity to small height changes.

For the analysis, the SAR data processing starts from the standard Coregistered Single-Look Slant-range Complex (CoSSC) product of each acquisition. The spatial resolution of the dual-pol images is 6.6 m in azimuth for all incidences, whereas in ground-range is 3.1 m for 22.7 degrees, 2.3 m for 30 degrees, and 1.8 m for 39 degrees. In all cases, the pixel spacing (pixel size) is around 2.4 m in both coordinates. It must be noted that TanDEM-X single-pol images present the same range resolution, but the azimuth resolution is 3.3 m, i.e. half the one in dual-pol case. The large spatial baselines that characterize the input data lead to a notable geometrical decorrelation derived from shifts in the wavenumber. Therefore, range spectral filtering is applied to compensate for this decorrelation. Then, a 21 $\times$ 21 boxcar filter was applied to the

This article has been accepted for publication in a future issue of this journal, but has not been fully edited. Content may change prior to final publication. Citation information: DOI 10.1109/JSTARS.2021.3100874, IEEE Journal of Selected Topics in Applied Earth Observations and Remote Sensing

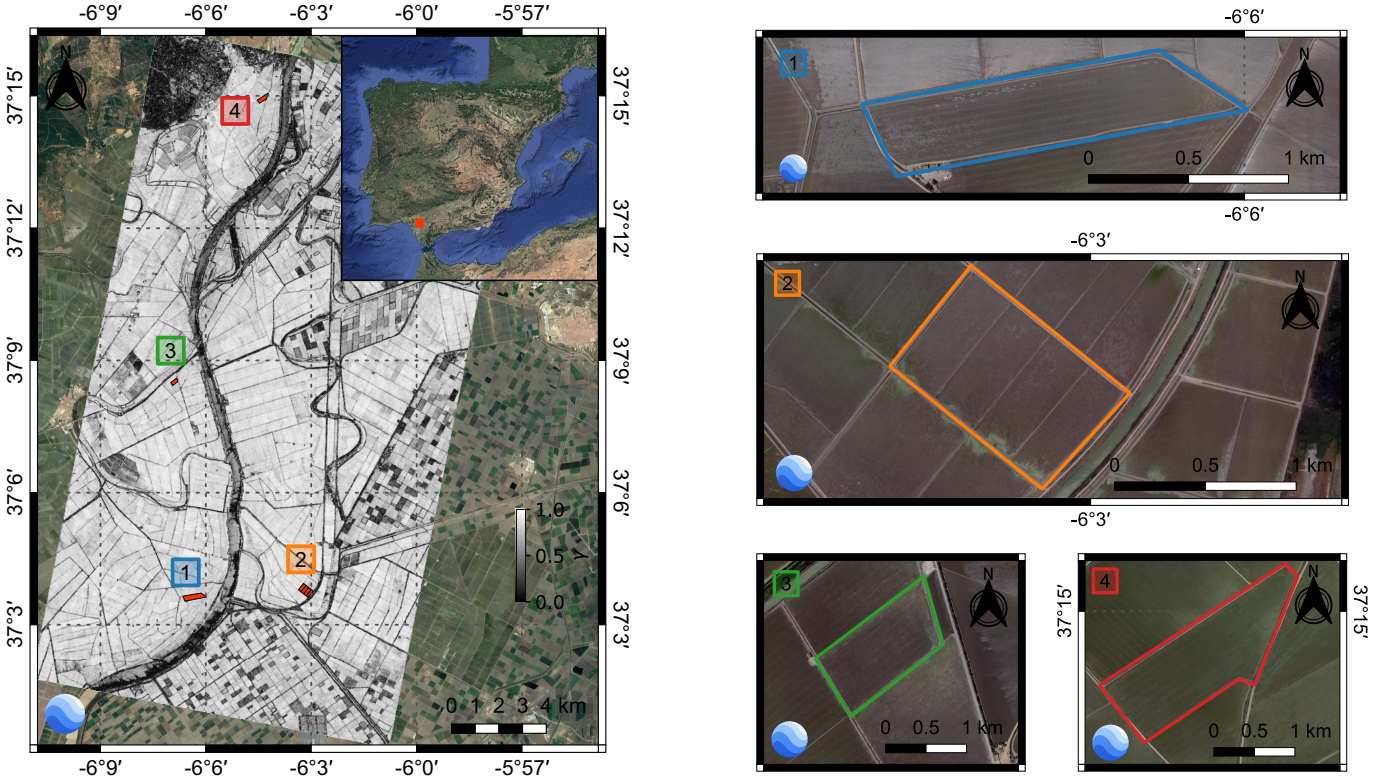

Fig. 1. On the left, the location of the test site in Sevilla (Spain), covering the entire area of 30 km × 30 km, is presented. Coherence amplitude of the VV channel acquired on June 26 2015 is shown. Location of the test fields of the ground campaign are highlighted and zoomed in on the right.

data for multi-looking. After the low-pass filtering, the spatial resolution is around 50 m in both directions. The flat Earth and topographic phase contributions were removed before forming the interferograms, so they are actually differential interferograms. This yields to an interferometric phase containing only topographic information with respect to an arbitrary phase reference (that was computed from the DEM). A 5 m grid size DEM provided by the Spanish National Center for Geographic Information (CNIG) [28] is used in this study.

III. InSAR Height Retrieval Methodologies

A. Single-pol InSAR methodologies

1) Common pre-processing. DEM calibration and ground phase estimation: Interferometric SAR methodologies are based on the exploitation of the complex interferogram [2]. Therefore, in some approaches a DEM calibration and an absolute phase retrieval are crucial pre-processing steps to estimate crop height from differential interferometric phases [29].

First, a DEM calibration is necessary to cancel the arbitrary phase value that appears in any interferogram. This phase offset term is constant for the whole interferogram, and is caused by the SAR processing of the image pair.

To this end, once the topographical component has been removed (i.e. input DInSAR data), for each date i in the time series, a stable target (e.g. bare surface) in which the height does not change and the phase is assumed to be constant over time is selected. The topographic phase for that stable point P is affected by the offset term as follows

$$\phi^P_{\text{ref},i} = \kappa^P_{Z,\text{ref},i} \cdot z^P_{\text{ref},i} + \phi^P_{\text{off},i}, \tag{2}$$

where $z^P_{\text{ref},i}$ is the height of the ground surface and $\phi^P_{\text{off},i}$ is the phase offset. Since the input data are differential interferograms, the phases at those points where the height is equal to that of the DEM are supposed to be zero. Thus, $\kappa^P_{Z,\text{ref},i} \cdot z^P_{\text{ref},i}$ is assumed null in the reference point. Consequently, $\phi^P_{\text{ref},i}$ in (2) is a measure of the phase offset term at point P:

$$\phi^P_{\text{ref},i} = \phi^P_{\text{off},i}. \tag{3}$$

Considering that the height at point P is constant over time, together with the fact that all data are processed with the same DEM, the process described above applies to all interferograms. For all dates, the phase is then calibrated with respect to the reference point:

$$\phi_{\text{cal},i} = \phi_i - \phi^P_{\text{ref},i}, \tag{4}$$

in which $\phi_i = \kappa_{Z,i} \cdot z_i + \phi_{\text{off},i}$, and $\phi^P_{\text{ref},i}$ as in (3) leads to

$$\phi_{\text{cal},i} = \kappa_{Z,i} \cdot z_i. \tag{5}$$

In (5), the arbitrary offset term present in all acquisitions has been removed. Hence, $\phi_{\text{cal},i}$, which is the phase of the measured coherence, is expected to be directly proportional to the height of the scattering center of the plants [30]. The resulting calibrated interferogram can be expressed as follows:

$$\Omega_{12,\text{cal},i} = \Omega_{12,i} \cdot \exp\left(-j\phi^P_{\text{ref},i}\right). \tag{6}$$

To test the performance of the DEM calibration, Fig. 2 shows an example of the temporal evolution of the reference point phase ϕ^P_{ref} and the calibrated phase ϕ_{cal}. Field 1 (see

This article has been accepted for publication in a future issue of this journal, but has not been fully edited. Content may change prior to final publication. Citation information: DOI 10.1109/JSTARS.2021.3100874, IEEE Journal of Selected Topics in Applied Earth Observations and Remote Sensing

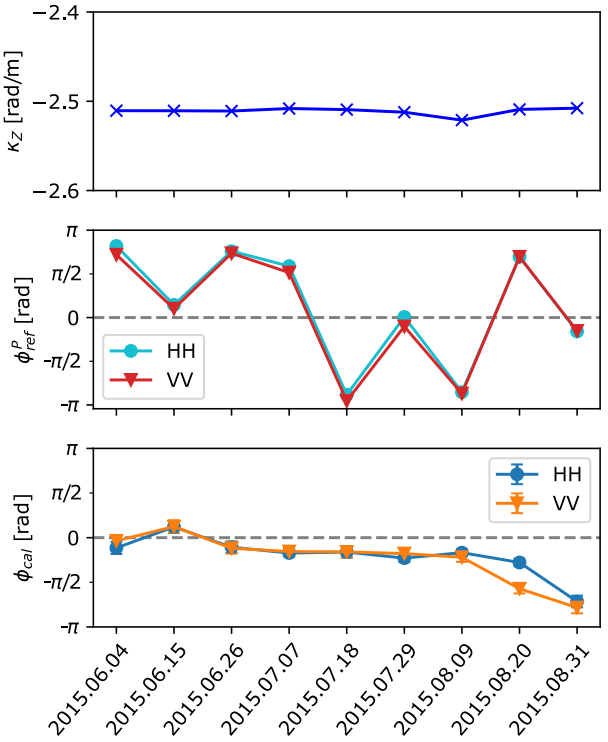

Fig. 2. Temporal evolution of the vertical wavenumber κ_Z, the phase of the reference point ϕ^P_{ref}, and the calibrated phase ϕ_{cal}. Results correspond to field 1 and 22.7 degrees of incidence angle. Average values are presented, and error bars denote ±one standard deviation, both computed for all pixels inside field 1.

Fig. 1) for a 22.7 degree acquisition (see Table I) has been selected.

The vertical wavenumber remains almost constant over time, around -2.5 rad/m. Thus, it does not affect the phase of the stable reference point. On the contrary, the phase of the reference point shows an arbitrary behavior due to the influence of the offset term. The calibration aims to get rid of this variability in all acquisitions. Indeed, the calibrated phase after removing the offset term does not show an arbitrary behavior but a decreasing trend along time (due to the negative sign of the κ_Z), with the exception of the second acquisition (June 15). The decrease in phase is more noticeable in the last three dates, especially for the VV polarimetric channel. These results corroborate the proportionality of the scattering phase center to height, thus ensuring a proper DEM calibration. The inversion with methodologies based on the interferometric phase (Sections III-A2 and III-A4) is only possible thanks to the proportional variation of the phase center with time. Prior to this calibration process, which, to our knowledge, is detailed here for the first time, the estimation of vegetation height based only on the interferometric phase is not possible. Unfortunately, the evolution of the calibrated phase in Fig. 2 does not show a large slope until the last two dates, which means that the vegetation height increase during July does not impact strongly the phase. Consequently, retrieval methods based on the phase are expected to underestimate the vegetation height during that period.

After the phase calibration, the second step is the ground phase estimation for each rice field. In single-pol inversion approaches, many studies have employed an external DEM to estimate the ground phase in forest scenarios [27], [31]–[33], and also in crop cases [8]. More recently, other studies have proposed to estimate the underlying topography without the use of external information. In such a case, flat topography is assumed in scenes characterized by a flooded condition, like mangroves [34] or rice fields [12]. Similarly to this latter study [12], the present work focuses on rice crops, and the ground phase is obtained directly from the calibrated interferogram. In the area under study, the fields are kept flooded during the entire cultivation period, until the maturation stage, when the fields are emptied to let crops dry. Thus, the ground is considered as a water surface from the radar point of view. In these circumstances, the reference ground topography is extracted from the first acquisitions at the early vegetative stages, right after the plants have emerged. These acquisitions are characterized by a high coherence thanks to the dominance of the double-bounce backscatter coming from the water-stems interaction. This usually corresponds to the first date of June available in the TanDEM-X time series (see Section II-B and Table I), denoted by i_0. Let P_C be a point in the center of the parcel under evaluation. The calibrated phase at that point for the selected date, i.e. $\phi^{P_C}_{\text{cal},i_0}$, is then the ground phase:

$$\phi_0 = \phi^{P_C}_{\text{cal},i_0}. \tag{7}$$

From this initial phase, the topography is obtained as follows:

$$z_0 = \phi_0 / \kappa^{P_C}_{Z,i_0}, \tag{8}$$

and it is used to correct the remaining acquisitions:

$$\Omega_{12,\text{corr},i} = \Omega_{12,\text{cal},i} \cdot \exp(-j z_0 \kappa_{Z,i}). \tag{9}$$

This interferogram, already calibrated and compensated by the topographic phase (9), is the input to the single-pol InSAR inversion methodologies.

Fig. 3 illustrates every step of the pre-processing for an area surrounding field 1 in the site. Data are presented for the VV polarimetric channel, since it has shown greater sensitivity to changes in the vegetation height, i.e. the scattering phase center is closer to the top of the canopy (see Fig. 2) [8]. The input interferometric coherence and phase are compared with the phase after DEM calibration and after topographic phase correction, respectively. In addition, the histogram of the phase calibrated and compensated by the topographic phase computed for all points inside the parcel is displayed.

The effect of the arbitrary phase offset term present in the input interferometric coherences is clearly visible, i.e. each acquisition presents a different dominant phase value. After the calibration, the offset term is removed, and the phases in which the height corresponds to that of the DEM are expected to be zero. The calibrated phases of the parcel under study (i.e. third column of Fig. 3), present a zero mean phase value, which predominates in the first acquisitions. This value gradually decreases as the plants start to grow, as it was also observed in Fig. 2. Comparing the interferometric coherence with the calibrated phase results, lower coherence levels produced by a growing volume decorrelation are also

This article has been accepted for publication in a future issue of this journal, but has not been fully edited. Content may change prior to final publication. Citation information: DOI 10.1109/JSTARS.2021.3100874, IEEE Journal of Selected Topics in Applied Earth Observations and Remote Sensing

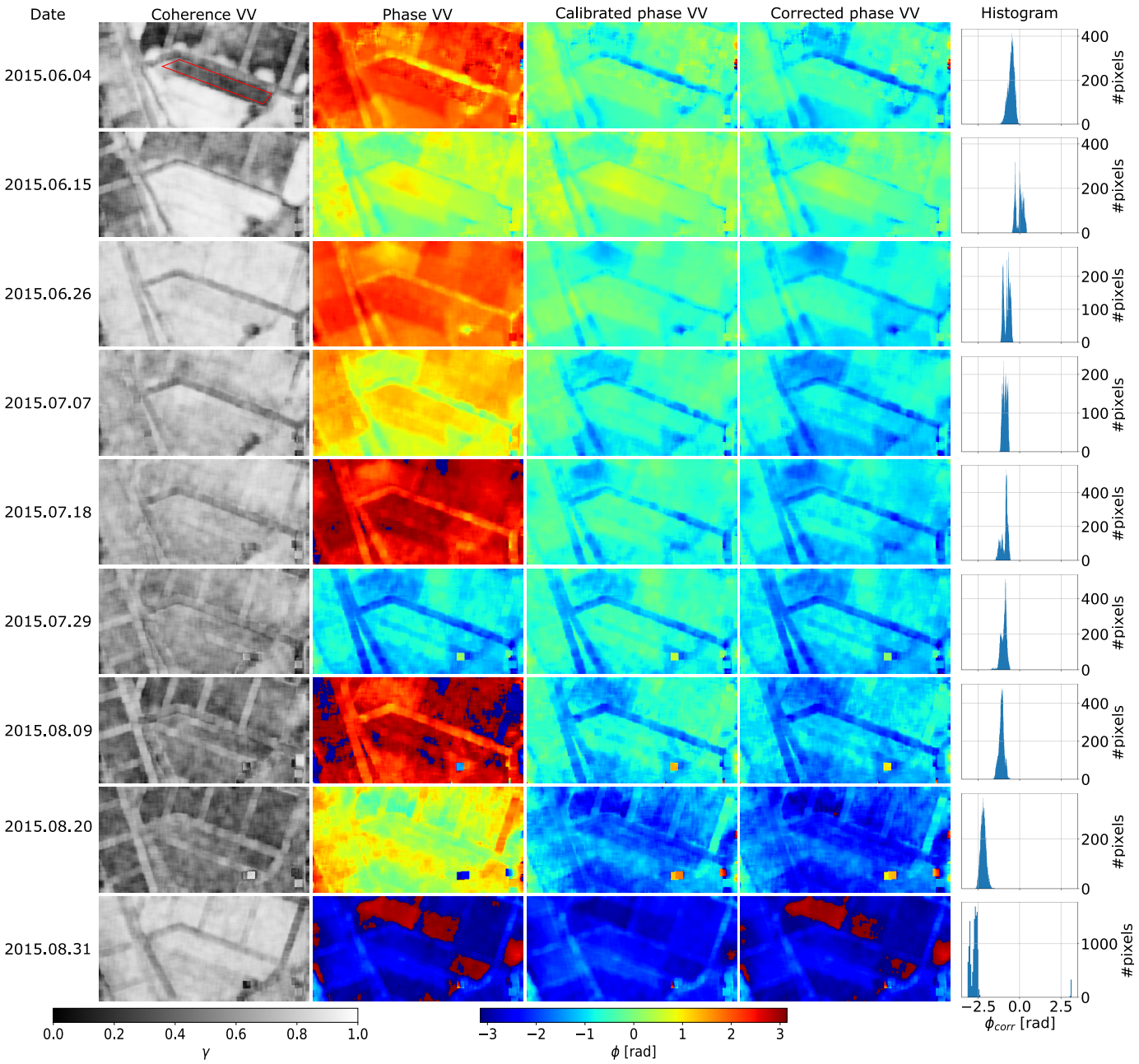

Fig. 3. Maps for the VV polarization channel in the area around field 1 (red polygon) in the Sevilla test site. From left to right the maps represent: interferometric coherence, phase before calibration, phase after calibration, and phase after calibration and topography correction. Histograms in the last column represent the calibrated and compensated phase of field 1. Results are shown for all TanDEM-X acquisitions at 22.7 degrees of incidence (9 dates).

related to a decreasing phase value. Once the topographic phase has been compensated, the difference between the phases of later acquisitions with respect to the ground phase correspond to changes in the vegetation height. These changes can be observed in the histograms of the last column. At the early stages of the growth cycle, i.e. at early June, the values within the parcels are around 0 rad. Then, as the plants start to grow, the predominant phase value decreases. Considering a negative κ_Z for 22.7 degrees, this decrease is associated with an increasing vegetation height. At the end of August, the dominant phase value is around -2.7 rad.

The phase histograms in Fig. 3 reveal that plants growth is not homogeneous within a field. The observed phase histograms do not correspond to an approximately Gaussian shape, as expected from a homogeneous area. This can be also observed in the phase images, where the left and right halves of the parcel have different dominant phase values. Accordingly, the histograms of the corrected phase exhibit a bimodal behavior at some dates, i.e. 15 and 26 June, 18 August and 31 September. This means that the growing rate, and thus, the height of the plants, is different at different parts of the same field. Since the ground-truth data provides a single average height value per field and date, this inhomogeneity adds uncertainty in the final vegetation height estimates.

2) Interferometric phase-based methodology: Rossi and Erten [8] demonstrated that the differential interferometric phase can be used to detect changes in vegetation height, and thus, to measure the evolution of rice height along time.

Taking as only input the phase of the interferogram properly calibrated and compensated, as in (9), a direct relationship with the vegetation height is established by the vertical wavenumber κ_Z (1). For each time series, the difference between heights extracted in subsequent images and the reference in (8) constitute the final vegetation height estimates.

The location of the phase center depends on the morphological properties of the canopy and its interaction with the radar signal. According to the penetration capability of the signal, the estimated height of the scattering phase center may differ from one polarimetric channel to another [8], [17]. Therefore, both TanDEM-X HH and VV channels are considered for the analysis.

3) Coherence amplitude-based methodology: Among the different InSAR and PolInSAR methodologies to retrieve vegetation parameters, the Random Volume over Ground (RVoG) [26], [35], [36] model is the most extended approach to link interferometric data (complex coherences acquired at any polarimetric channel) to scene parameters (topographic phase, vegetation height, extinction, and ground-to-volume ratios). Based on this model, the vegetated scene is composed of two layers: a homogeneous volume layer of randomly oriented scatterers on top of an impenetrable ground layer. The scattering from the volume is distributed according to a vertical reflectivity function $f(z)$ of thickness h_v, whereas the scattering from the ground is located at a single point $z = z_0$.

The RVoG model can be simplified in order to use the interferometric coherence amplitude as a single input parameter for height retrieval. This approach has been widely used for forest height estimation using single-polarization TanDEM-X data [15], [16]. For a feasible inversion, extinction in the vegetation volume and the ground-to-volume ratio at the available polarimetric channel need to be fixed. Therefore, the inversion allows for the estimation of only one model parameter, i.e. vegetation height. The simplest assumption consists in null extinction and null ground contribution, which leads to the following SINC model:

$$|\tilde{\gamma}| = |\tilde{\gamma}_V| = \text{sinc}\left(\frac{\kappa_Z h_v}{2}\right), \tag{10}$$

where h_v is the vegetation height, $\tilde{\gamma}$ is the measured coherence, and $\tilde{\gamma}_V$ is the coherence due to the vegetation volume alone.

The inversion is then carried out following two main steps. The first step is the compensation of the nonvolumetric decorrelation contributions [6]. After range spectral filtering (Section II-B), the main nonvolumetric decorrelation in bistatic TanDEM-X mode is the additive noise, γ_{SNR}. For each polarization channel, it is defined by the signal-to-noise ratio (SNR) at each pixel [27]. Moreover, the decorrelation due to data quantization γ_{BAQ} [37] is taken into consideration as well [9]. The SINC function is then inverted using the following approximate expression to provide height estimates [15], [16]:

$$h_v \approx \frac{2\pi}{\kappa_Z}\left(1 - \frac{2}{\pi}\sin^{-1}|\tilde{\gamma}_V|^{0.8}\right). \tag{11}$$

Another possibility to invert the RVoG model consists in assuming known values of extinction and ground-to-volume ratio. The inversion is then carried out by minimizing the distance between the measured coherence and the model. The expressions of the general RVoG model coherence and the minimization problem are shown later in Section III-A4.

4) Complex coherence-based methodology: When both interferometric phase and coherence amplitude are used for the inversion, the complex coherence constitutes the input data to the retrieval algorithm [12]. The RVoG model provides the expression of the coherence $\tilde{\gamma}$ at a polarization channel $\vec{w}$ as

$$\tilde{\gamma}(\kappa_Z, \vec{w}) = e^{i\phi_0}\frac{\tilde{\gamma}_V + \mu(\vec{w})}{1 + \mu(\vec{w})}, \tag{12}$$

where $\phi_0 = \kappa_Z z_0$ is the topographic phase and $\mu(\vec{w})$ is the ground-to-volume ratio at a specific polarization. The term $\tilde{\gamma}_V$ is the coherence of the volume layer, without any ground contribution. According to the vertical reflectivity function $f(z)$, it is expressed as follows:

$$\tilde{\gamma}_V = \frac{\int_0^{h_v} f(z)e^{i\kappa_Z z}dz}{\int_0^{h_v} f(z)dz}. \tag{13}$$

The single-pol inversion methodology in (12) is unbalanced with only one measured complex coherence $\tilde{\gamma}(\kappa_Z, \vec{w})$ (i.e. two real input data) and four unknowns: topographic phase ϕ_0, vegetation height h_v, extinction σ and ground-to-volume ratio $\mu(\vec{w})$. Thus, in order to design a feasible inversion strategy adapted to the observation space, additional assumptions are required. First, the ground phase is estimated directly from the TanDEM-X interferogram acquired during the early stages of the growth cycle, as described in Section III-A1. Second, the contribution from the ground is assumed null, i.e. $\mu(\vec{w}) = 0$. Therefore, with this method one can estimate both vegetation height h_v and extinction σ.

Similarly to Section III-A3, the inversion is carried out following the steps of compensation of nonvolumetric decorrelation contributions and inversion of the RVoG model for the retrieval of parameters. In this case, the inversion is based on a numerical minimization of the distance between the compensated measured coherence $\tilde{\gamma}(\kappa_Z, \vec{w})$ and the modelled volume coherence $\tilde{\gamma}_V$:

$$\min_{h_v, \sigma} \left\| \tilde{\gamma}(\kappa_Z, \vec{w}) - \tilde{\gamma}_V e^{i\phi_0} \right\|. \tag{14}$$

B. Dual-pol InSAR methodology

When more than one polarimetric channel is available, PolInSAR approaches can be applied to the inversion of the RVoG model [27], [9]. In the most general case, the response from the ground can be composed of two contributions, i.e. a direct scattering and a double-bounce scattering. In that case, the complex coherence from expression (12) is expressed as follows:

$$\tilde{\gamma}(\kappa_Z, \vec{w}) = e^{i\phi_0}\frac{\tilde{\gamma}_V + \mu_D(\vec{w}) + \gamma_{DB}\mu_{DB}(\vec{w})}{1 + \mu_D(\vec{w}) + \mu_{DB}(\vec{w})}, \tag{15}$$

where $\mu_D(\vec{w})$, $\mu_{DB}(\vec{w})$ are the ground-to-volume backscatter ratios corresponding to the direct (D) and double-bounce

(DB) contributions, respectively. The first factor in the third term of the numerator in (15), γ_{DB}, is the double-bounce decorrelation term that appears whenever a bistatic configuration is used. It is defined as

$$\gamma_{DB} = \frac{\sin\left(\kappa_Z \sin^2\theta_0 h_v\right)}{\kappa_Z \sin^2\theta_0 h_v}, \tag{16}$$

and its influence is thoroughly analyzed in [20]. Depending on the dominant ground contribution, the expression in (15) simplifies to (12), either considering $\mu_D(\vec{w})$ or $\mu_{DB}(\vec{w})$. In the present work, for the sake of comparison with the rest of methodologies, the simplest case of a dominant direct ground contribution is considered.

The inversion strategy by means of PolInSAR approaches usually consists of three main steps. First, a line fit to the coherence region and selection of the coherences with minimum and maximum ground contribution, $\tilde{\gamma}(\kappa_Z, \vec{w}_{\text{min}})$ and $\tilde{\gamma}(\kappa_Z, \vec{w}_{\text{max}})$, is carried out to estimate the underlying topography [27]. Note that in this case, there is no need to estimate or calibrate in advance the topographic phase, i.e. the PolInSAR inversion itself provides its estimate. The second and third steps are analogous to those described in Sections III-A3 and III-A4: compensation of nonvolumetric decorrelation sources and numerical estimation of model parameters. This latter step is carried out by an iterative minimization of the distance between the measured extreme complex coherences $\tilde{\gamma}(\kappa_Z, \vec{w})$ and the modeled ones $\tilde{\gamma}$:

$$\min_{h_v,\sigma,\mu_{\text{max}},\mu_{\text{min}}} \left\| \begin{bmatrix} \tilde{\gamma}(\kappa_Z, \vec{w}_{\text{max}}) e^{-i\phi_0} \\ \tilde{\gamma}(\kappa_Z, \vec{w}_{\text{min}}) e^{-i\phi_0} \end{bmatrix} - \begin{bmatrix} \tilde{\gamma}(\kappa_Z, h_v, \sigma, \mu_{\text{max}}) \\ \tilde{\gamma}(\kappa_Z, h_v, \sigma, \mu_{\text{min}}) \end{bmatrix} \right\|, \tag{17}$$

The numerical inversion of the dual-pol InSAR methodology provides the estimates of all RVoG model parameters, i.e. vegetation height h_v, extinction σ, and ground-to-volume ratios μ_{min} and μ_{max}.

IV. Results

This section presents the results from the aforementioned theoretical methodologies obtained from the TanDEM-X data set described in Section II-B (Table I).

With the purpose of inspecting the input data sets, and to support the interpretation of height estimates retrieved later with the different InSAR methodologies, the measured coherence is presented first. The temporal evolution of the mean coherence over the selected fields (see Fig. 1) is illustrated in Fig. 4 for all incidence angles. Please note that field 4, which is located at the North end of the scene, is outside the footprint of the data acquired with 30 degrees of incidence. To ease the understanding of the coherence levels of Fig. 4, colored backgrounds show, in average, the different growing stages. It is important to bear in mind that transitions between growing stages are slightly different from one field to another. Hence, Fig. 5 presents the specific phenology calendar according to the BBCH scale of each monitored field. In addition, complementary information of the rice growth cycle is represented in Fig. 6. Each growing stage is associated with its respective BBCH scale values, plant morphology and dominant scattering mechanism.

During the first acquisitions in May (DoY $<$ 150), the parcels are characterized by a bare rough surface without plants or water, which translates into a strong backscatter and high coherence. In Fig. 4, this is reflected in the first two acquisitions for 30 degrees of incidence, i.e. May 4 and 15. As observed in Fig. 5, May 15 (DoY 135) is the first sowing date, corresponding to field 3. Then, until mid June (150 $<$ DoY $<$ 170), transitioning between early and late vegetative stages, the flooded ground reflects the incident signal in a specular direction, yielding low returns to the SAR antenna. Plants are absent or have just emerged from the water surface (as Fig. 6 depicts), and the coherence is very low, e.g. 0.37 coherence level at the first acquisition in field 1 for 22.7 degrees. At the end of June, still during the early stages of the growth cycle, the interaction of the incident wave with short rice plants and flooded ground results in a predominant double-bounce scattering mechanism. A high level of coherence is derived from a very localized radar response at the water surface level. From this date onward, the coherence starts to decrease. This is observed for DoY $>$ 180, approximately. Moreover, due to the different attenuation at the two polarization channels, the decreasing trend is usually more pronounced at the VV channel than at the HH one [17], [9]. In late July and early August (DoY $>$ 220), between the early and late reproductive stages, when plant height is around its maximum value, the strong attenuation produces very low backscatter and, hence, low coherence levels. Finally, in late August and early September (DoY $>$ 240), high coherence values are reached again. The drier and more random morphology of the plants, characteristic of late reproductive stages and initial maturative ones, reduces the attenuation in the volume.

For the later analysis of the vegetation height estimates, it is important to acknowledge a higher overall coherence level at 22.7 degrees than at 30 and 39 degrees. The reason for this is the longer path followed by the signal at shallower incidence angles, which translates in a larger attenuation.

Another feature worth considering is that while at 22.7 and 39 degrees the earliest high coherence values (after flooding) are observed at mid June, for field 1 at 30 degrees they are not found until June 28. The reason for this is the time of acquisition: the orbit passes at 22.7 and 39 degrees are descending, whereas the orbit passes at 30 degrees are ascending. Descending images are acquired at 6:30 h in the morning, and ascending images at 18:15 h. Observing the fifth acquisition at 30 degrees, which corresponds to June 17 (DoY 168), the wind was strong (5 m/s) precisely at 18:30 h. On the contrary, on June 15 at 6:30 h the wind was less than 2 m/s. A similar situation is observed for 39 degrees. Observing the second acquisition on June 10 (DoY 161), the wind speed at 6:30 h is around 2.5 m/s. Although the wind is not as strong as around the same date for 30 degrees, Fig. 4 still shows a slightly lower level of input coherence at field 1 compared to that of the remaining fields. A wind stronger than 3 m/s generates a noticeable roughness in the water surface if there is only water, or water with plants of low height and density. Hence, the direct backscattering from the rough

This article has been accepted for publication in a future issue of this journal, but has not been fully edited. Content may change prior to final publication. Citation information: DOI 10.1109/JSTARS.2021.3100874, IEEE Journal of Selected Topics in Applied Earth Observations and Remote Sensing

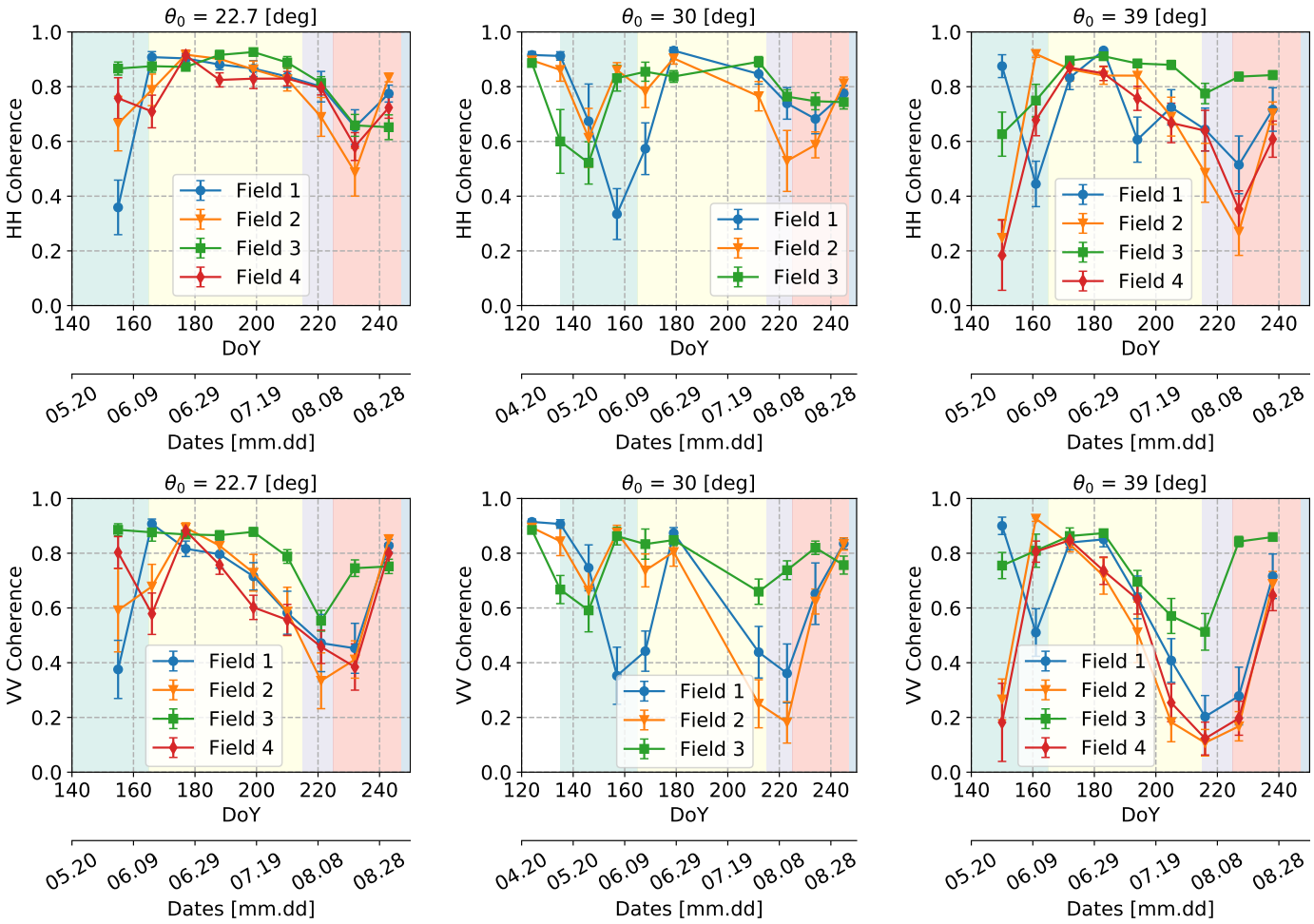

Fig. 4. Temporal evolution of the total measured coherence after range spectral filtering for the HH (upper row) VV (bottom row) polarization channels obtained for all monitored fields in Sevilla. From left to right results are shown for 22.7, 30 and 39 degrees of incidence angle. Average values are presented, and error bars denote ±one standard deviation. Colored backgrounds correspond, in average, to a different growing stage according to the BBCH scale: early and late vegetative, early and late reproductive, and maturative stages.

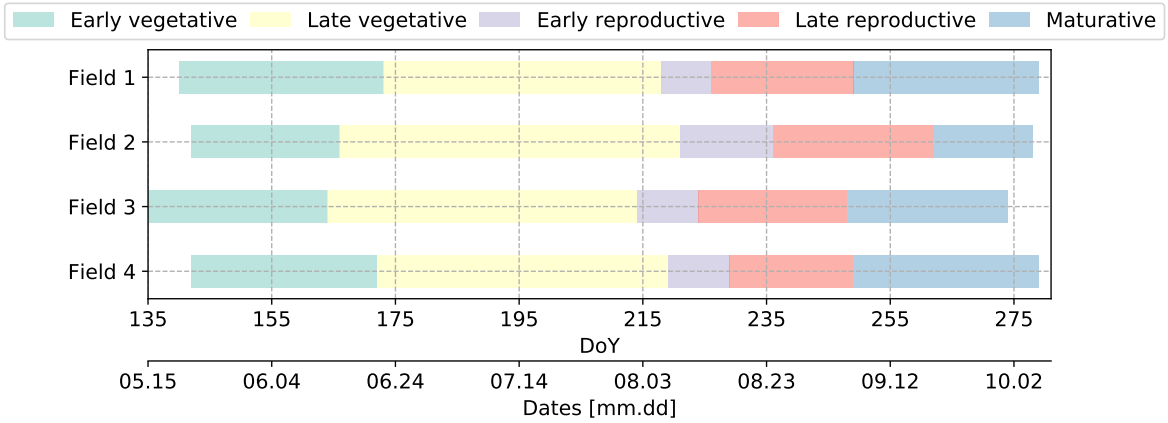

Fig. 5. Crop phenology calendar according to the BBCH scale of the four monitored fields.

surface increases, and the specular scattering decreases, which is the one that generates the double-bounce. As a consequence, the received signal is weak and the resulting coherence value is very low in field 1 in that situation.

A. Results from the interferometric phase-based methodology

A direct comparison with the reference ground-truth data is employed in order to assess the accuracy of the crop height estimation methodologies. Fig. 7 shows the temporal evolution of the vegetation height estimates obtained from the methodol-

This article has been accepted for publication in a future issue of this journal, but has not been fully edited. Content may change prior to final publication. Citation information: DOI 10.1109/JSTARS.2021.3100874, IEEE Journal of Selected Topics in Applied Earth Observations and Remote Sensing

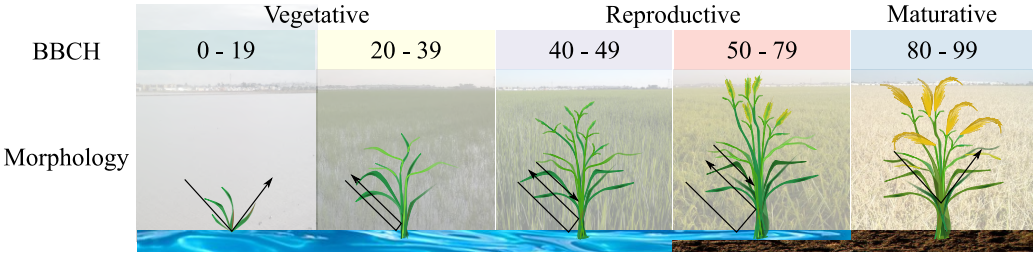

Fig. 6. Growth cycle of rice with the corresponding BBCH scale and the dominant scattering mechanisms at each growing stage.

ogy based on the interferometric phase (Section III-A2). From left to right, each column corresponds to the four monitored fields, whereas each row presents the results for the different incidence angles available (Table I). Vegetation heights are retrieved on the grounds that the interferometric phase is directly proportional to the height of the scattering phase center. The location of the phase center is normally below the top of the canopy, since the SAR signal penetrates into the vegetation volume [38]. Therefore, height estimates are expected to be below field measurements. In this approach, DEM calibration and absolute phase estimation (Section III-A1) are key steps to measure vegetation height from the interferometric phase.

According to the measured input coherence (shown in Fig. 4), the reference ground phase is estimated from the first acquisition, after flooding, in which a sufficient coherence level ensures a reliable phase estimate [12]. This depends on the phenological stage of each field at the dates of acquisition (see Fig. 5) and on the TanDEM-X system configuration (baseline and incidence angle). Table II specifies the reference date from which the ground phase has been estimated for each field at each incidence. For 22.7 degrees, the ground phase is extracted from the second or third acquisition, June 15 and 26, respectively. Similarly, for 39 degrees, it is also possible to find reliable phase estimates in mid June, around June 10 and 21, but the ground reference is taken from the fourth acquisition (July 2) for fields 1 and 3. From June 21 to July 2, the coherence slightly increases until it starts decreasing at that point, e.g. for the HH channel at field 1 the coherence level goes from 0.86 to 0.93. A more detailed analysis deserves the scenario observed at 30 degrees. As mentioned before, images at 30 degrees of incidence are acquired in an ascending orbit at 18:15 h, whereas images at 22.7 and 39 degrees are acquired in a descending orbit at 6:30 h. In this case, different acquisition times imply a variation of weather conditions. In this latter case, on June 17 a wind of 5 m/s yields low coherence levels, thus preventing us from extracting a reliable phase estimate. As a consequence, the ground phase is estimated on June 28 for fields 1 and 2. Since vegetation heights are retrieved from the difference between heights extracted in subsequent images and the reference ground phase, valid estimates are obtained only from the reference date onward, which may be different from field to field [12].

Vegetation height estimates presented in Fig. 7 for all fields and incidences are underestimated. In general, the first acquisitions do not exhibit a good correspondence with field measurements, since the difference between the measured

TABLE II
REFERENCE GROUND PHASE

Incidence angle	Field	Reference date (DoY)
22.7 degrees	Field 1	2015.06.15 (166)
	Field 2	2015.06.26 (177)
	Field 3	2015.06.15 (166)
	Field 4	2015.06.26 (177)
30 degrees	Field 1	2015.06.28 (179)
	Field 2	2015.06.28 (179)
	Field 3	2015.06.06 (157)
39 degrees	Field 1	2015.07.02 (183)
	Field 2	2015.06.10 (161)
	Field 3	2015.07.02 (183)
	Field 4	2015.06.21 (172)

phase and the ground phase is not enough to reflect any noticeable crop growth. Only for DoY $>$ 200 (June 19), i.e. during the late vegetative stage, the phase appears to be sensitive to vegetation height. In addition, attending to the crop growth cycle and the associated properties of the canopy (e.g. plant water content, structure and density), HH and VV signals experiment different levels of attenuation, showing discrepancies between their associated height estimates [8], [17], which are also more evident for DoY $>$ 200 (July 19). Since the double-bounce contribution predominates more at HH than at VV, the phase center at HH is closer to the ground. Instead, phases closer to the top of the canopy are observed at VV channel [39]. As a result, the height estimates at the VV channel are closer to the real values. Later on, in late August and early September (i.e. transitioning to the maturative stage, around DoY 240), plants are more randomly oriented and drier (as observed in Fig. 6). This condition yields a more similar response in both polarizations, and almost all fields at all incidences produce nearly identical estimates in the last acquisition.

The variability of the results within the fields, i.e. the observed standard deviation shown by means of error bars in Fig. 7, is lower for the HH than for the VV channel. In addition, it is higher for shallower incidences. It is worth recalling the phase histograms in Fig. 3, which corroborate the inhomogeneity of the plants growth within a field. In the last date, August 31, the bimodal behavior of the histogram is due to phase wrapping because the actual crop height is close to HoA/2, so the phase is close to π. In this specific situation, a correction of one cycle is performed over the phase before

This article has been accepted for publication in a future issue of this journal, but has not been fully edited. Content may change prior to final publication. Citation information: DOI 10.1109/JSTARS.2021.3100874, IEEE Journal of Selected Topics in Applied Earth Observations and Remote Sensing

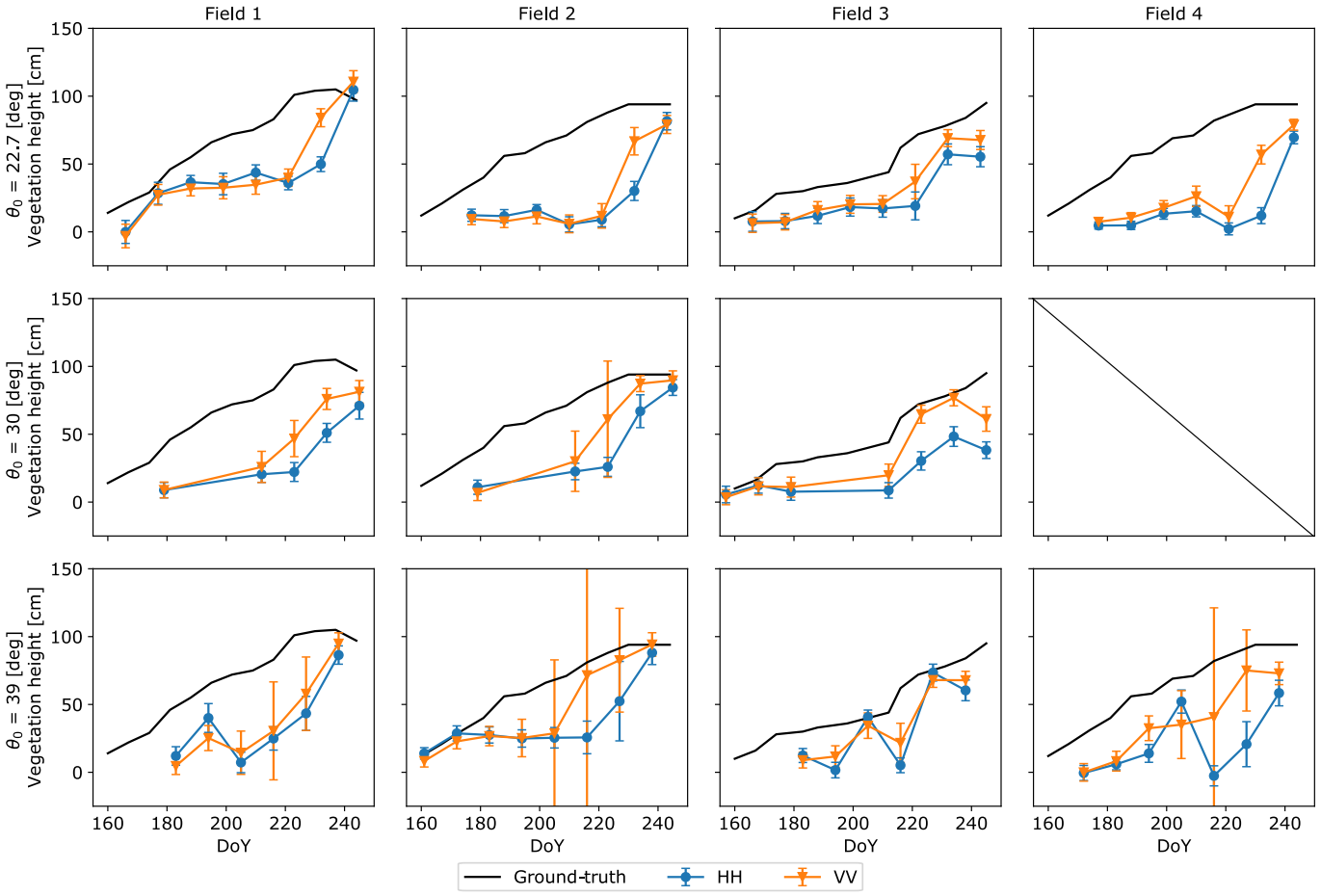

Fig. 7. Temporal evolution of the vegetation height estimates of HH (blue) and VV (orange) channels and ground-truth data (black) for the monitored fields in Sevilla. Estimates are obtained following the interferometric phase-based methodology (Section III-A2). Average values are presented, and error bars denote ±one standard deviation.

the height inversion, i.e. $\pm 2\pi$ is added to the phase (depending on the vertical wavenumber sign) before the height estimation.

At 39 degrees of incidence, the large standard deviation observed on August 4 (DoY 216) in fields 1, 2 and 4 in the VV channel is due to a very low coherence level (below 0.2). This is associated with a very noisy phase, which yields high variability in the vegetation height estimates. Fig. 8 shows the coherence and phase at this date for field 2. The low coherence level achieved at VV, together with a very noisy phase, compared to that of HH, is obvious. To quantitatively illustrate the differences between the phases of both channels, Fig. 9 presents the histograms of the phase employed for inversion. With such a noisy input phase observed at VV channel, providing accurate estimates with a methodology based only on the interferometric phase is not possible.

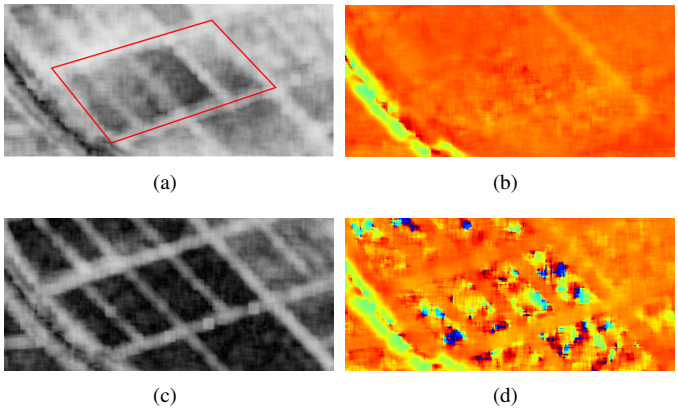

Fig. 8. Coherence and phase maps corresponding to the HH, (a) and (b), and VV, (c) and (d), polarization channels for field 2 (red square). Results are acquired at 39 degrees of incidence angle on August 4 (DoY 216).

B. Results from the coherence amplitude-based methodology

The temporal evolution of the vegetation height estimates obtained from the methodology based on the coherence amplitude (Section III-A3) is displayed in Fig. 10. Since the input to the inversion methodology is the coherence amplitude alone, the DEM calibration and ground phase estimation (Section III-A1) do not affect the final estimates.

A common behavior for all incidences is that as the coherence decreases due to an increasing volume decorrelation for growing plants, the height estimates follow a increasing temporal trend. However, the higher input coherence observed at 22.7 degrees is reflected in the final estimation accuracy,

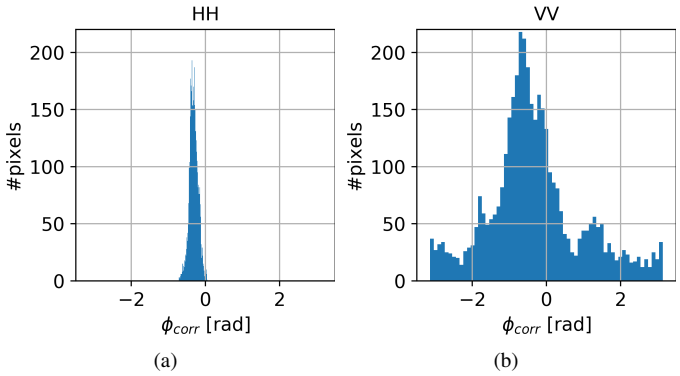

Fig. 9. Histograms of the interferometric phase of field 2 after the pre-processing steps of DEM calibration and interferogram correction (Section III-A1) employed as input to the inversion. Results are acquired at 39 degrees of incidence angle on August 4 (DoY 216).

since results for 22.7 degrees are more accurate than those for 30 and 39 degrees. Considering the coherence amplitude as only input, a better estimation accuracy of the HH channel is obtained compared to the VV, which is observed in Fig. 4 and it was also noted by Erten *et al.* in [17]. The higher values of coherence at the HH channel translate into a smaller standard deviation, similarly to the results for the interferometric phase-based methodology (Fig. 7). Considering the results for all the different incidences, heights estimated in field 3 present a better correspondence to *in-situ* measurements than those obtained in the other parcels.

Since the extinction and the ground contribution are assumed null following the SINC model in (10), the retrieved heights are overestimated when the input coherence is lower than the modelled one. Such an overestimation is more visible for shallower incidences in the VV channel, especially when plants are around 1 m tall (i.e. 210 $<$ DoY $<$ 230, approximately). In order to provide an insight on this issue, Fig. 11 illustrates how much the physical model adapts to the input data, as well as how the assumptions made in the model (i.e. null extinction and ground-to-volume ratio) affect this adaption. Considering data for field 2, for each angle of incidence and polarization channel, the measured coherence (after the corresponding compensations) is presented. It is then compared with the coherence expected by the physical model when taking as input the available ground-truth height under different assumptions: (a) null extinction and null ground contribution, (b) null extinction but non null ground response, and (c) both extinction and ground response different from zero.

Among the different assumptions considered in the model, the one that best suits the measured data is option (c), which corresponds to non null extinction through the vegetation volume (σ = 5 dB/m) and non null response from the ground (μ = 1). Moreover, it is evident that the model adapts best to the input data at 22.7 degrees, for which the coherence expected by the model is closest to the coherence provided by the TanDEM-X data. In contrast, advancing in the growing season the measured coherence decreases more than the expected one, a feature which is even more pronounced for the VV channel. Very low input coherence values (below 0.3) are affected by a biased and noisy estimation, so even after the SNR compensation [27] the coherence is not high enough to provide reliable height estimates. The strongly biased results observed for field 2 at 30 and 39 degrees in Fig. 10 are explained by the mismatch between model and data, since the model, under any of the evaluated assumptions, produces so low coherence values. These results clarify also the overestimation observed in Fig. 10 in other cases, e.g. fields 1 and 4 at 30 and 39 degrees.

C. Results from the complex coherence-based methodology

The next methodology under study is based on the interferometric complex coherence (Section III-A4). In this methodology, both interferometric phase and coherence amplitude are employed in the inversion. Hence, DEM calibration and ground phase estimation (Section III-A1) are necessary pre-processing steps. The reference ground phase is retrieved following the procedure described above for the interferometric phase-based methodology, according to the reference dates specified in Table II. Vegetation height estimates obtained following this approach are displayed in Fig. 12.

Results from the interferometric phase-based approach (Fig. 7) exhibited a general underestimation, whereas results from the coherence amplitude-based methodology (Fig. 10) were, on the whole, overestimated (especially for the shallowest angles). The joint use of coherence amplitude and interferometric phase is expected to balance these two opposite behaviors and provide more accurate vegetation height estimates.

As it has been anticipated, when the input coherence is high enough and the phase is stable within the parcel and along time, vegetation height estimates obtained using the interferometric complex coherence are more accurate than using only the phase or the amplitude. Thus, results for field 1 at 22.7 degrees and field 3 at all incidences have improved considerably compared to the results of the previous two methodologies. The trends observed are similar to those obtained following the interferometric phase-based approach (Fig. 7), but more accurate and less underestimated. On the other hand, due to the problems of low coherence level and high phase variability of the input data, vegetation height estimates at 30 and 39 degrees for fields 2 and 4 are strongly biased. This is particularly noticeable in the VV channel. As explained before, the great difference observed in the VV channel compared to the HH comes from the lower coherence value at VV, with an associated high phase variability (see Fig. 8). In this case, the increasing trend of the vegetation height estimates along time is similar to that followed by the results of the coherence amplitude method (Fig. 10). However, the estimates are less overestimated due to the influence of the interferometric phase in the retrieval.

To illustrate the mismatch between the physical model of the scene and the input data, the example of field 2 at 39 degrees is considered for a deeper analysis. Fig. 13 compares the measured input coherence employed for inversion (after the compensation of decorrelation sources) versus the

This article has been accepted for publication in a future issue of this journal, but has not been fully edited. Content may change prior to final publication. Citation information: DOI 10.1109/JSTARS.2021.3100874, IEEE Journal of Selected Topics in Applied Earth Observations and Remote Sensing

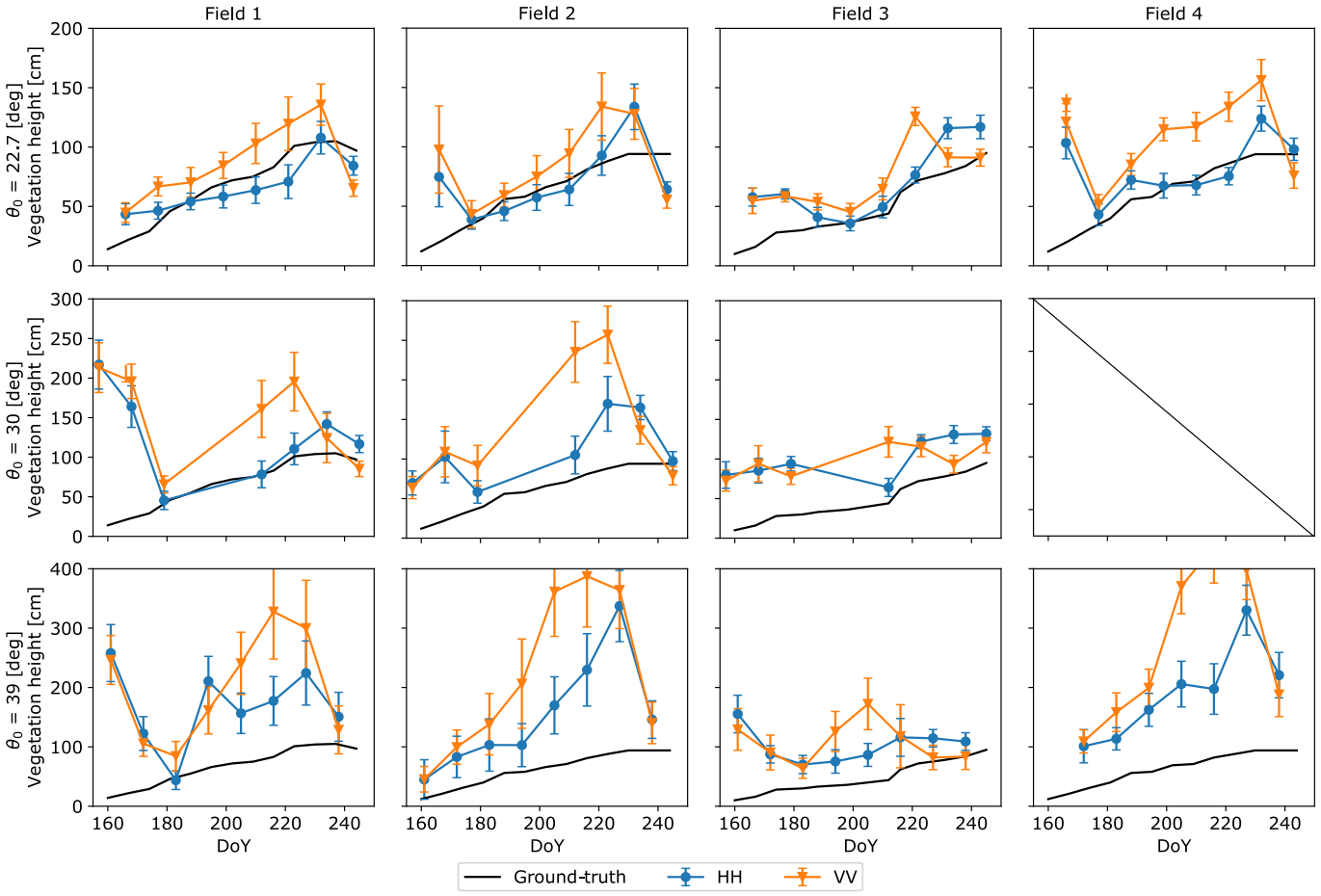

Fig. 10. Temporal evolution of the vegetation height estimates of HH (blue) and VV (orange) channels and ground-truth data (black) for the monitored fields in Sevilla. Estimates are obtained following the coherence amplitude-based methodology (Section III-A3). Average values are presented, and error bars denote ±one standard deviation.

interferometric complex coherence of the RVoG model, as in (12) and (13). Again, the differences between channels HH and VV are observed at first sight. For the HH channel, vegetation heights for the first six acquisitions are relatively well estimated, up to August 4 (DoY 216), and only the last two present a higher overestimation, which is reflected in a larger separation of the coherence points on the complex plane. Except for the acquisition of August 15 (DoY 227), the rest of acquisitions show a mean coherence value above 0.8. On the contrary, a different scenario is observed for the VV channel. Only in the first four acquisitions, until July 13 (DoY 194), the height estimates are accurate enough. Up to that point, the mean coherence level is above 0.8, and therefore, the model is able to adjust to the input data. On the complex plane, we can observe how for the first four dates, coherence points, both from the input data and the model, are close to the unit circumference. However, from the fifth acquisition onward, i.e. July 24 (DoY 205), the coherence drops to lower levels, reaching minimum values below 0.4. In those cases, the model still expects coherence levels close to 1, and therefore, is not able to adjust to the input data. The reason behind this decrease in the VV channel, which has been previously discussed, is the strong attenuation due to the vertical arrangement of the plant elements. Since this is a recurrent problem in all the methodologies studied so far, favoring the HH channel over the VV seems reasonable when assessing crop height from bistatic data for the central growth stages. This goes in line with the findings of Erten *et al.* in [17] regarding the polarization impact on paddy rice height estimation with TanDEM-X data. Other scenarios in which a great mismatch between estimates and real data is observed, e.g. field 2 at 30 degrees or field 4 at 39 degrees, are explained similarly. The low input coherence level and high phase variability achieved at the VV polarization makes the physical model of the scene unable to fit the real data, thus resulting in strongly biased estimates.

These results indicate that the vegetation height estimation employing the interferometric complex coherence suffers from the problems associated with low input coherence level and high phase variability. Very low coherence levels (below 0.3) imply a large phase variance despite using a large multi-look (i.e. 21×21). In these cases, as observed in Section IV-A in Figs. 8 and 9, the phase is too noisy to be properly estimated. In addition, the SNR correction only modifies the coherence amplitude, whereas the phase remains as noisy as it was in the beginning. Therefore, even if the SNR compensation

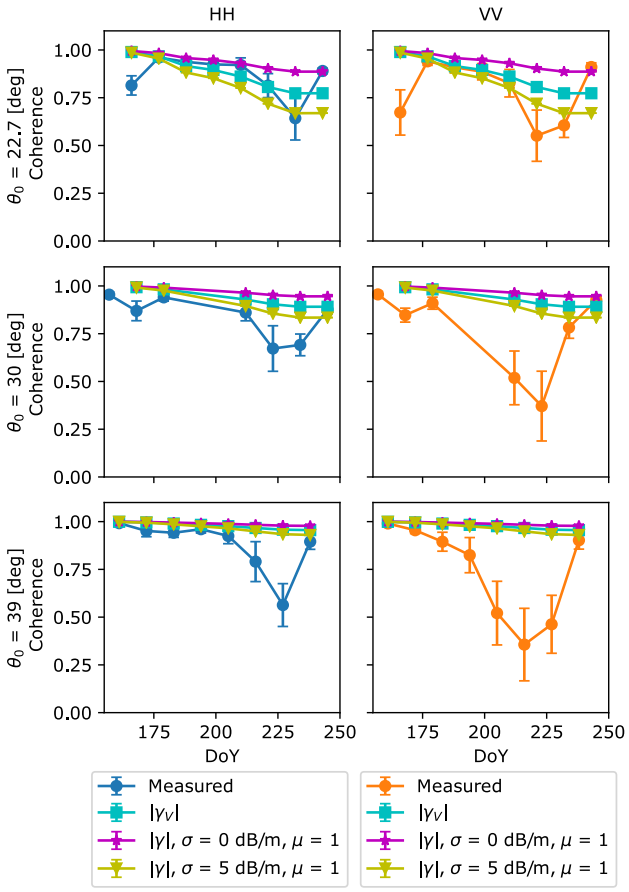

Fig. 11. Measured input coherence employed for inversion (blue for HH and orange for VV), compared with the coherence amplitude of the RVoG model under different assumptions: (a) null extinction and null ground contribution (10) (cyan), (b) only null extinction, i.e. considering the coherence amplitude of (12) with (10) (magenta), (c) without simplifying the RVoG model, i.e. considering the complex coherence amplitude from (12) and (13) (yellow). Data corresponds to field 2.

increases the coherence amplitude, this is not enough to ensure a correct inversion. This was also observed when analyzing the results of the coherence amplitude-based methodology (Section IV-B).

D. Results from the PolInSAR methodology

Up to this point, results for single-pol InSAR methodologies have been presented. Now, results obtained by means of a dual-pol InSAR methodology (Section III-B) are analyzed. Fig. 14 shows the vegetation height estimates obtained with this approach. Since the PolInSAR inversion itself provides a topographic phase estimate, there is no need to perform the pre-processing steps of DEM calibration and ground phase estimation (Section III-A1).

Overall, PolInSAR vegetation height estimates at steep incidences, i.e. 22.7 degrees, are quite accurate, and the results are better than many of the previous methodologies. However, this scenario changes for shallower incidences, i.e. 30 and 39 degrees. Compared to the results of the interferometric phase-based methodology (Fig. 7), for these shallower incidences, the overestimation present at PolInSAR estimates is larger than the mismatch observed at the interferometric phase-based results. Regarding the vegetation height estimates obtained using only the coherence amplitude (Fig. 10), one may find several similarities with the results of the VV channel. Although heights retrieved with PolInSAR are generally less overestimated, an important overestimation is still present owing to very low coherence levels taken as input to the inversion. On the other hand, results at HH polarization of the coherence amplitude-based methodology exhibit better accuracy in some cases, such as field 1 at 30 degrees. This suggests that the low coherence obtained at the VV channel has also an impact on the PolInSAR estimates. At last, estimates retrieved from the complex coherence-based methodology (Fig. 12) reveal similar trends, but with some exceptions (e.g. field 3 at 30 and 39 degrees). PolInSAR-based estimates perform better than those obtained at the VV channel when inverting using the complex coherence. In this sense, compared to the results of the VV channel in which the interferometric phase is an input (i.e. interferometric phase- and complex coherence-based methodologies), PolInSAR estimates show less standard deviation. Therefore, the effect of high phase variability at 30 and 39 degrees is somehow compensated. However, heights obtained at the HH polarization are considerably more accurate than the PolInSAR estimates. As mentioned earlier, at incidences of 30 and 39 degrees, larger HoA and smaller vertical wavenumber (Table I) lead to less interferometric sensitivity to the vertical distribution of the scatterers in the vegetation volume. This translates into an overestimation clearly visible in the PolInSAR estimates. Moreover, such an overestimation is larger when the product of vegetation height and vertical wavenumber is very small, i.e. for $h_v < 30$ cm (DoY < 180). On the contrary, in methodologies based on the difference between heights from subsequent images with respect to the ground phase, i.e. interferometric phase- and complex coherence-based methodologies, this overestimation is counteracted. As a consequence, the accuracy of the final estimates is slightly better in these approaches than in PolInSAR for 30 and 39 degrees.

E. Comparison of InSAR methodologies

Validation plots between height estimates and field measurements for all methodologies under study are shown in Fig. 15. A quantitative comparison is carried out between average inversion height per field and date against ground-truth data. Columns 1–4 present the results for each methodology under evaluation, whereas rows 1–3 correspond to the different incidence angles. This representation supports previous comments concerning the trends observed in the estimated heights for the different methodologies. In general, coherence amplitude- and PolInSAR-based methodologies show an overestimation of the vegetation height, which is particularly noticeable at shallower incidences (30 and 39 degrees). On the other hand, interferometric phase- and complex coherence-based methodologies present a more pronounced underestimation. As also noted by several authors [40], [9], [12], for very short vegetation (i.e. $<$ 30–50 cm, approximately), Fig. 15 reveals that a lack of interferometric sensitivity together with

This article has been accepted for publication in a future issue of this journal, but has not been fully edited. Content may change prior to final publication. Citation information: DOI 10.1109/JSTARS.2021.3100874, IEEE Journal of Selected Topics in Applied Earth Observations and Remote Sensing

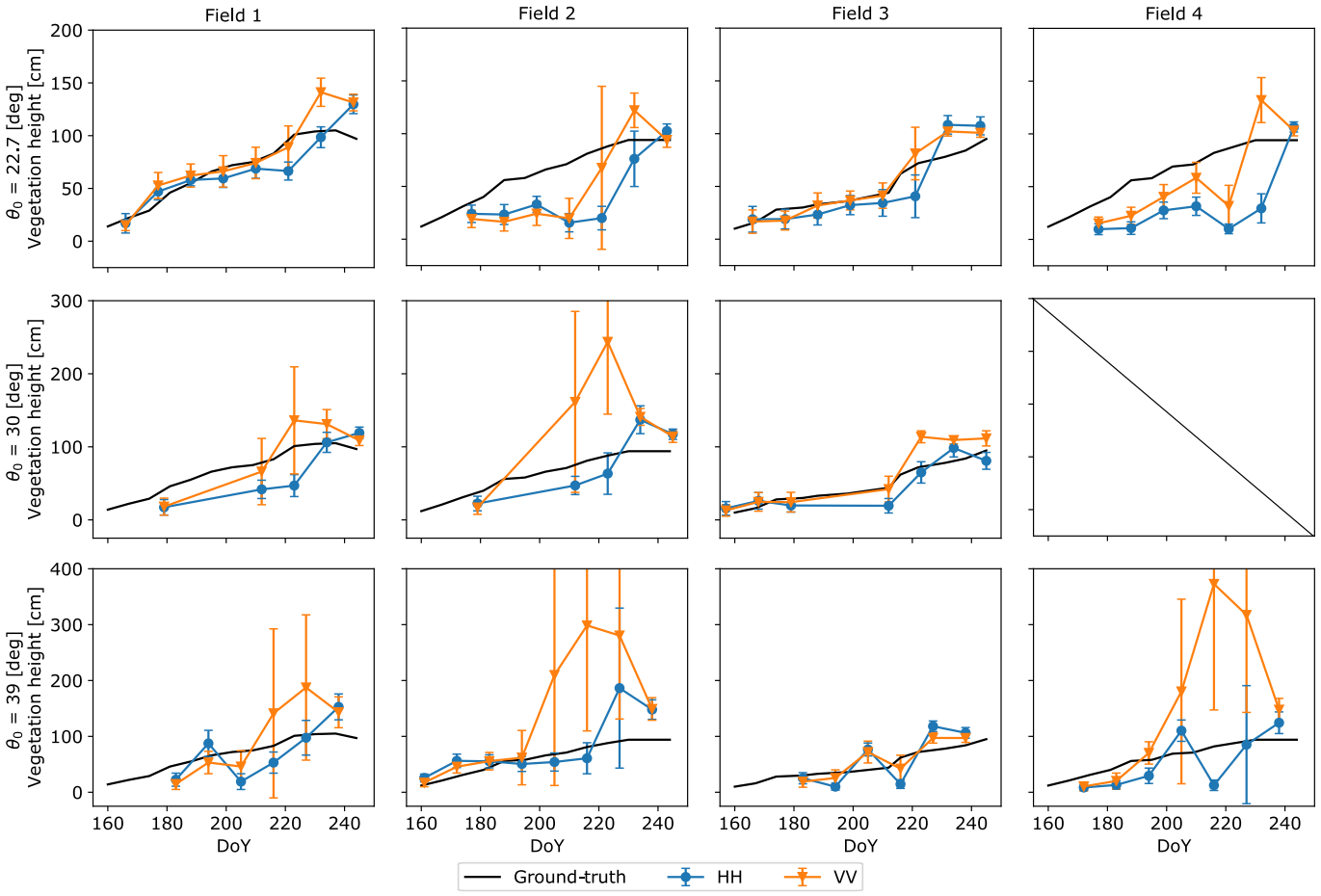

Fig. 12. Temporal evolution of the vegetation height estimates of HH (blue) and VV (orange) channels and ground-truth data (black) for the monitored fields in Sevilla. Estimates are obtained following the complex coherence-based methodology (Section III-A4). Average values are presented, and error bars denote ±one standard deviation.

small residual non-volumetric decorrelation result in large height errors. Therefore, in order to provide suitable short vegetation height estimates, larger effective spatial baselines than the ones available in the current data set (Table I) should be used. According to this criterion, statistics presented in Table III are computed for the range of estimates in which field measurements are above 25 cm. In the end, the accuracy analysis is conducted over n = 28, 15 and 26 measurements for 22.7, 30 and 39 degrees, respectively.

As expected from the observations of Fig. 15, coherence amplitude- and PolInSAR-based methodologies obtain clearly better results for steep incidences than for shallower ones. Thus, a correlation coefficient R^2 of 0.61 and 0.45 for HH and VV polarization with the coherence amplitude method, and 0.48 with PolInSAR, are obtained at 22.7 degrees. These results correspond to the lowest root-mean-square errors (RMSE): 17, 31, and 23 cm, respectively. In contrast, R^2 decreases and RMSE increases at 30 and 39 degrees of incidence. Values of 0.51 and 0.13 for HH and VV with the coherence amplitude method, and 0.11 with PolInSAR, are found at 30 degrees. These values are associated with the smallest correlation that can be observed in the entire data set. Moreover, although the correlation at 39 degrees

TABLE III
STATISTICS OF THE CORRELATION BETWEEN HEIGHT ESTIMATES AND FIELD MEASUREMENTS

Incidence angle	Methodology	Polarization channel	R^2	RMSE [cm]
22.7 degrees (n = 28)	Phase-only	HH, VV	0.31, 0.51	46, 39
	Coherence amplitude	HH, VV	0.61, 0.45	17, 31
	Complex coherence	HH, VV	0.39, 0.64	33, 25
	PolInSAR	HH–VV	0.48	23
30 degrees (n = 15)	Phase-only	HH, VV	0.52, 0.69	45, 31
	Coherence amplitude	HH, VV	0.51, 0.13	42, 76
	Complex coherence	HH, VV	0.62, 0.56	27, 52
	PolInSAR	HH–VV	0.11	54
39 degrees (n = 26)	Phase-only	HH, VV	0.34, 0.69	41, 31
	Coherence amplitude	HH, VV	0.47, 0.27	106, 175
	Complex coherence	HH, VV	0.45, 0.48	37, 101
	PolInSAR	HH–VV	0.22	128

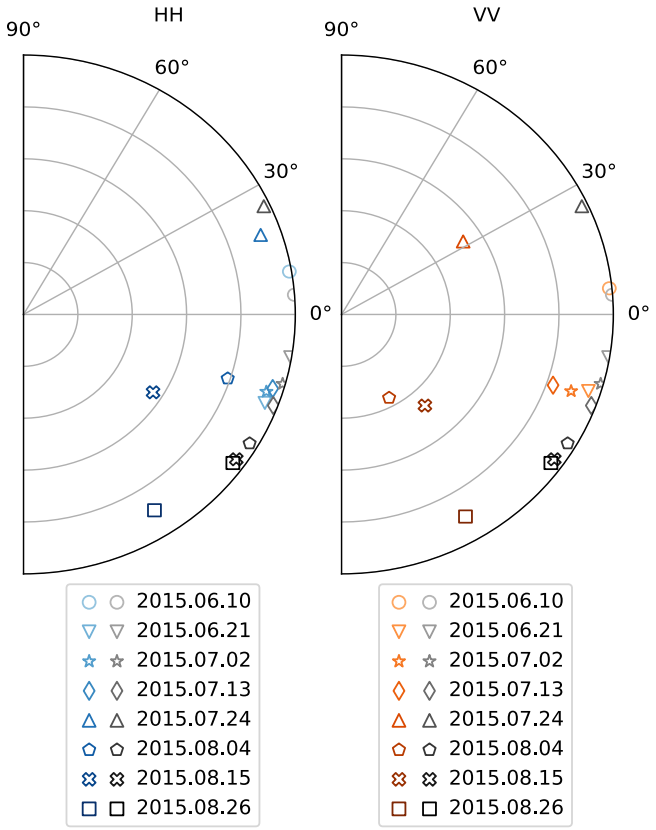

Fig. 13. Measured input coherence employed for inversion (shades of blue for HH and orange for VV) compared with the interferometric complex coherence of the RVoG model, using (12) and (13) (shades of black). Data corresponds to field 2 at 39 degrees of incidence.

increases for these methodologies, the largest RMSE are also found: 106 and 175 cm following the coherence amplitude methodology, and 128 cm employing PolInSAR. At these shallower incidences, Fig. 15 highlights an important overestimation in the estimates of the coherence amplitude and the PolInSAR method when plants are around 1 m high. For the interferometric phase-based methodology, in which the DEM calibration and ground phase estimation (Section III-A1) are performed prior to the inversion, a different situation arises. While relatively low determination coefficients, 0.31 and 0.51, are found for HH and VV channels at 22.7 degrees, incidences of 39 degrees disclose larger R^2 values, around 0.34 and 0.69 for each channel, respectively. It is evident that the accuracy of the interferometric phase-based methodology increases for larger incidences (as observed in Fig. 7) thanks to a longer path followed by the SAR signal into the vegetation volume. This explains the decrease in the RMSE from 46 and 39 cm for HH and VV at 22.7 degrees, to 41 and 31 cm at 39 degrees. However, as depicted in Fig. 15, a better correlation between estimates and ground data is not that evident for shallower incidences with the method based on the complex coherence. Due to the effect of low input coherence at large incidences (see Fig. 12), cases such as field 2 and 4 at 39 degrees yield important mismatches at the VV polarization that produce greater errors. Thus, although for the HH channel the correlation increases from 0.39 to 0.45, the RMSE also increases for both polarizations, i.e. from 33 and 25 cm at 22.7 degrees, to 37 and 101 cm for 39 degrees. Despite these errors, interferometric phase- and complex coherence-based methodologies yield better results at larger incidences than coherence amplitude- and PolInSAR-based approaches. On the contrary, better results are achieved at steep incidences with methodologies based on the coherence amplitude and PolInSAR.

As a final comparison, Fig. 16 presents maps of heights estimated with all the methodologies under study in a large area covering the entire test site. A date corresponding to the reproductive stage, when rice plants are around 1 m tall is selected, i.e. August 8 (DoY 232). Moreover, results are presented for 22.7 degrees of incidence, for which high enough input coherence is ensured, together with low HoA and large vertical wavenumber (i.e. 2.53 m and 2.48 rad/m). Each column presents the results from each methodology, and each row corresponds to the polarization channel evaluated, respectively. Pre-processing steps of DEM calibration and ground phase estimation are carried out on a parcel-by-parcel basis. Spatial homogeneity within the the whole area is observed. Thus corroborating the suitability of the inversion methodologies to large scale applications. General observations of previous results apply when studying this large area. Methods based on the interferometric phase and complex coherence (i.e. columns 1 and 3) provide underestimated results. In addition, this underestimation is larger at the HH channel than at VV, and more noticeable for the interferometric phase-based methodology than for the complex coherence-based methodology, with height values below 50 cm in many fields. On the other hand, methodologies based on the coherence amplitude and PolInSAR (i.e. columns 2 and 4) present greater vegetation height estimates. In particular, results from the coherence amplitude-based approach are around 1–1.5 m. The overestimation detected in previous analysis (see Fig. 10) is more noticeable in the VV channel, for which heights are predominantly around 1.5 m. Regarding the PolInSAR-based methodology, the results corroborate the suitability of this method for the retrieval of vegetation height when the conditions of steep incidence, associated with low HoA, are met. Under these circumstances, enough sensitivity to the distribution of the scatterers within the scene, and therefore, enough sensitivity to height, is ensured. Accordingly, the vast majority of fields reflect height estimates around 1 m.

V. Discussion and Conclusions

This work presents a comparison of all known InSAR techniques for the retrieval of rice crop height using TanDEM-X data sets. The assessment of the polarization influence on crop monitoring is carried out through the separate analysis of the available polarization channels, i.e. HH and VV. For this purpose, methodologies based on the interferometric phase, coherence amplitude, complex coherence, and PolInSAR, are studied. The performance of these methodologies is evaluated by a comparison with field measurements obtained during a ground campaign in 2015. The study of these approaches is completed by estimating crop height with different values of incidence angle and baseline.

This article has been accepted for publication in a future issue of this journal, but has not been fully edited. Content may change prior to final publication. Citation information: DOI 10.1109/JSTARS.2021.3100874, IEEE Journal of Selected Topics in Applied Earth Observations and Remote Sensing

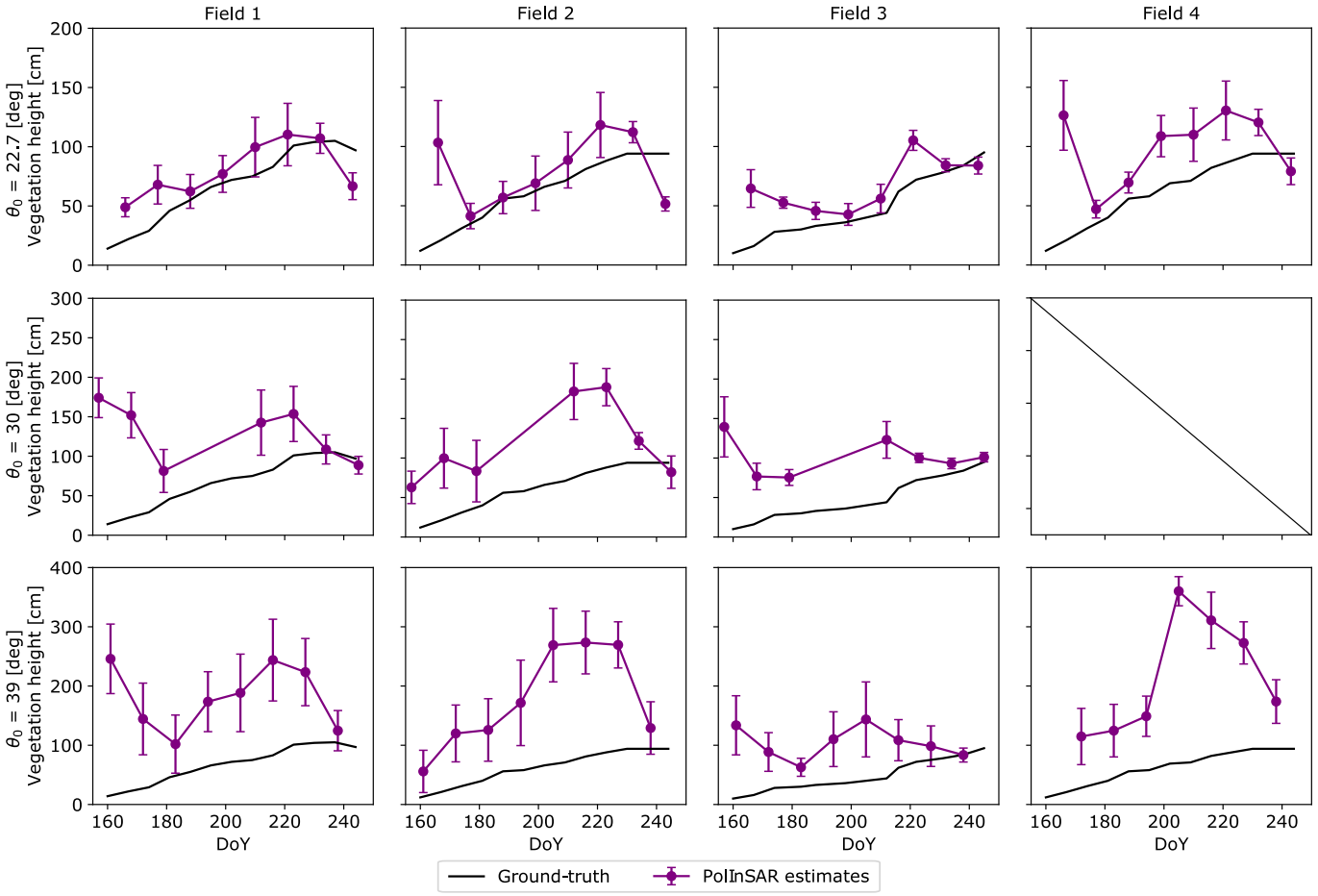

Fig. 14. Temporal evolution of the vegetation height estimates (purple) and ground-truth data (black) for the monitored fields in Sevilla. Estimates are obtained following the dual-pol InSAR methodology (Section III-B). Average values are presented, and error bars denote ±one standard deviation.

When employing the interferometric phase as single model input, the phase center is expected to be below *in situ* measurements [40]. This shows in the vegetation height estimates, which reveal the different penetration capability of each polarization channel. Corroborating observations of previous studies [8], [17], [1], height estimates are generally underestimated. However, the underestimation is more pronounced in the HH channel, for which the phase center is closer to the ground. The absolute accuracy of height estimates is better for VV polarized acquisitions, since the scattering is located closer to the top of the canopy. Nevertheless, VV results are strongly affected by very noisy phases at shallower incidences. With the exception of field 3, in which a relatively high accuracy is observed throughout the whole season at all incidences, valid height estimates (i.e. with a relative mean error (RME) below 10%) are only obtained for the VV channel for DoY > 220, from reproductive stages onward. Therefore, as stated in [17], when inverting using only the interferometric phase, having reliable coherence levels are not directly related to more accurate estimates. A drawback from this methodology is that an external vegetation-free DEM is required to retrieve plant height. This implies the need for the pre-processing steps of DEM calibration and absolute ground phase estimation. Moreover, the accuracy of the final estimates is affected by the accuracy of the external DEM.

With respect to the coherence amplitude-based methodology, the difference between height estimates from different polarization channels is even more noticeable. Considering the coherence amplitude as only input under the assumptions of null extinction and null ground contribution produces a clear overestimation of crop height. Indeed, VV signal estimates are less accurate than HH ones, especially for shallower incidences. These results are strongly affected by the measured input coherence level. When it is very low (e.g. below 0.3), the SNR correction does not provide coherence levels suitable for a reliable height estimation. Thus, valid estimates with an RME $< 10\%$ are found for the HH channel at all fields at 22.7 and 30 degrees, and only at field 3 at 39 degrees (i.e. due to its overall higher input coherence level, as observed in Fig. 4).

The combined problems of having very noisy phases, together with very low coherence levels as input data, are reflected in the results of the complex coherence methodology. This method shows a good performance when the simultaneous conditions of having a relatively high measured coherence and small HoA (large spatial baseline) are met. Otherwise, results show large standard deviations and important overestimations. Again, this is mainly observed in the VV channel.

This article has been accepted for publication in a future issue of this journal, but has not been fully edited. Content may change prior to final publication. Citation information: DOI 10.1109/JSTARS.2021.3100874, IEEE Journal of Selected Topics in Applied Earth Observations and Remote Sensing

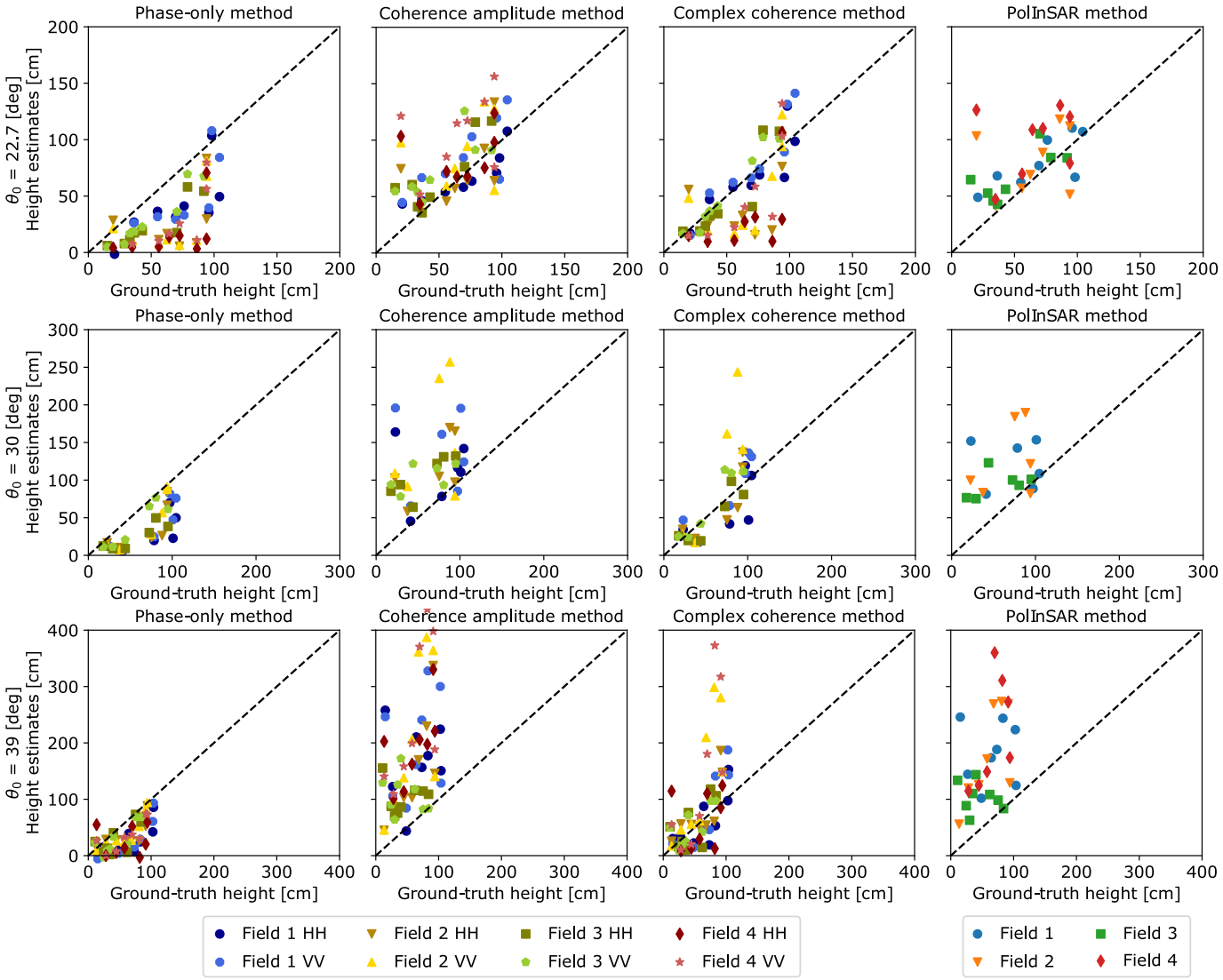

Fig. 15. Comparison of the average height estimates of the monitored fields in Sevilla obtained with the methodologies under evaluation. Each row shows the results for 22.7, 30 and 39 degrees of incidence angle, whereas each column present the results of the specific methodology.

Hence, valid height estimates (i.e. RME below 10%) are found for fields 1 and 3 at all incidences, but not for fields 2 and 4, in which the issues of noisy phases and low coherence levels are more pronounced. In the end, a compromise in terms of input coherence level is required. In order to see changes in height, volumetric decorrelation is needed (i.e. $|\tilde{\gamma}_V|$) [41]. This means that the input coherence needs to decrease along time, since decorrelation increases as plants grow. Nevertheless, a minimum coherence level is required to guarantee that signal power is greater than noise power and thus, that the SNR correction provides a feasible coherence level for inversion. In addition, the SNR compensation only improves the coherence amplitude, but noisy phases associated with low coherence levels remain the same. In a practical application, the measured coherence values should be higher than the ones observed in the current data set at 30 and 39 degrees of incidence. A solution to this combined problem would be to mask or discard the pixels in which the measured input coherence is below a certain threshold, e.g. 0.3. This could be further analyzed in future studies.

At last, the methodology based on PolInSAR suffers too from the problems described above. However, height estimates at shallower incidences show less standard deviation than in previous methods. This may be explained by the fact that the topography is provided by the inversion itself, which suggests that the effect of having noisy phases is counteracted with this method. On the other hand, there is an evident degradation of the estimates accuracy as we move to shallower incidences. This degradation is related to an increase of HoA (i.e. from 2.53 m at 22.7 degrees to 5.81 m at 39 degrees) and a decrease of the measured coherence level. In this case, valid height estimates (i.e. RME $<$ 10%) are achieved for all fields at 22.7 degrees, and only for field 3 at 30 and 39 degrees. In contrast to the rest of methodologies, the PolInSAR approach requires dual-polarized acquisitions for inversion. Finally, as in the coherence amplitude-based methodology, an external DEM is not required.

Table IV summarizes the main advantages and limita-

This article has been accepted for publication in a future issue of this journal, but has not been fully edited. Content may change prior to final publication. Citation information: DOI 10.1109/JSTARS.2021.3100874, IEEE Journal of Selected Topics in Applied Earth Observations and Remote Sensing

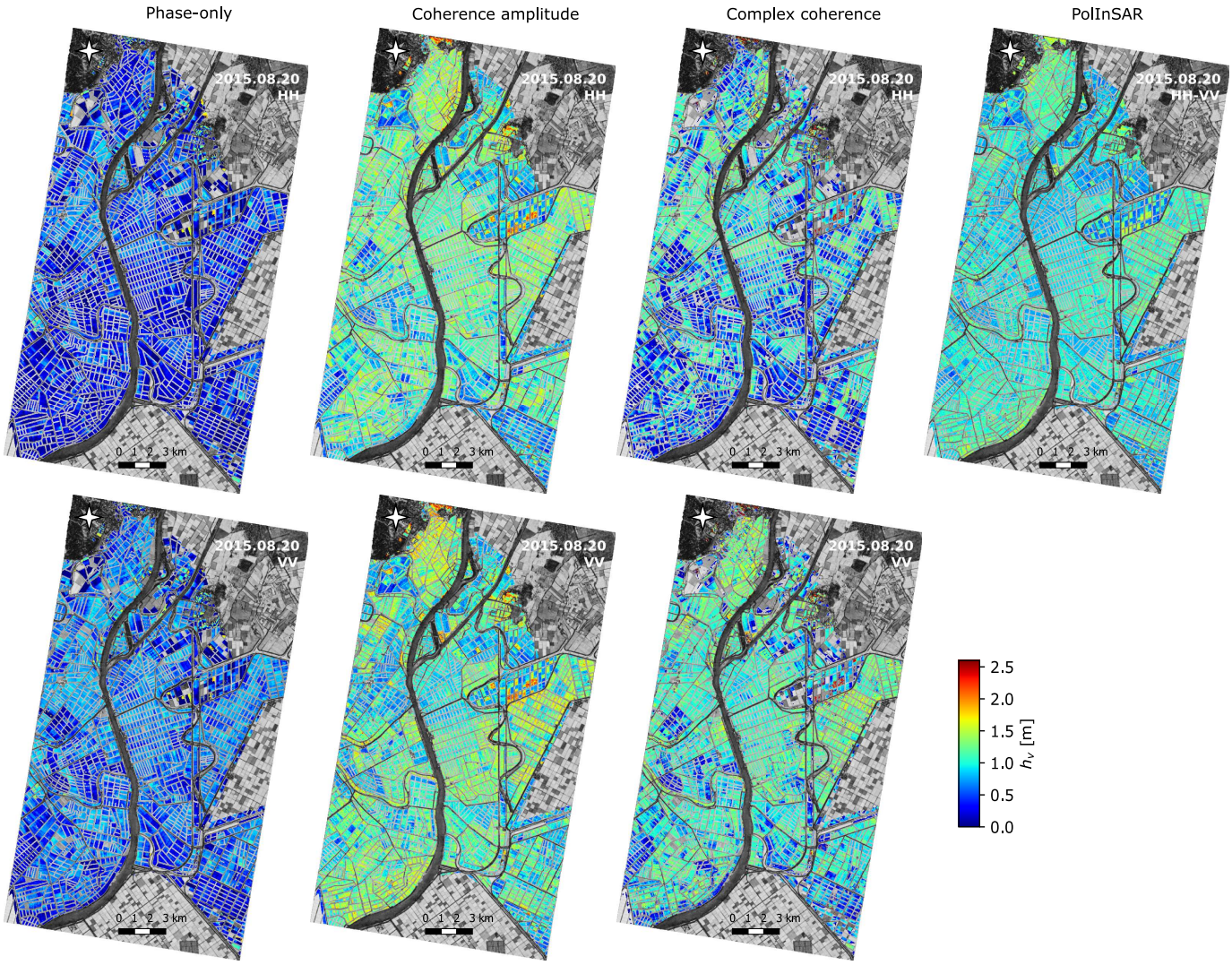

Fig. 16. Height maps around a large area of the Sevilla test site. Each row presents the height estimates of each polarization channel, and each column corresponds to the methodologies under evaluation, based on: interferometric phase, coherence amplitude, complex coherence and PolInSAR. An acquisition during the reproductive stage, August 8 (DoY 232), is selected. Results are presented for 22.7 degrees of incidence angle.

TABLE IV
ADVANTAGES AND DRAWBACKS OF THE INSAR METHODOLOGIES FOR THE RETRIEVAL OF RICE CROP HEIGHT

Methodology	Required acquisitions	External information	Advantages	Disadvantages
Phase-only	Single polarized	DEM free of vegetation	Computational cost Performs better at shallower incidences	Need for external DEM Underestimates vegetation height Suffers from noisy phases
Coherence amplitude	Single polarized	-	Computational cost No need for external data Performs better at steep incidences	Overestimates at shallower incidences Suffers from low input coherence
Complex coherence	Single polarized	DEM free of vegetation	Performs well at all incidences for suitable measured coherence values	Need for external DEM Suffers from noisy phases Suffers from low input coherence
PolInSAR	Dual polarized	-	No need for external data Performs well at steep incidences	Computational cost Overestimates at shallower incidences Suffers from low input coherence Large baseline needed Half swath (reduced coverage)

tions of the four approaches under evaluation, with focus on the requirements for consistent crop height monitoring. Although under suitable initial conditions, the dual-pol PolInSAR method is expected to provide the most accurate estimates, the better azimuth resolution and wider swath (i.e. larger spatial coverage) provided by single-pol data, makes them of great interest. In this sense, promising results have been obtained with single-polarized acquisitions in methodologies based on the coherence amplitude and on the complex coherence, which deserve further study.

To conclude, Fig. 17 presents the final vegetation height estimates obtained from the best combination of all methods. The method which shows the best performance at each acquisition date is selected as optimum, i.e. the method which provides the estimates with minimum absolute error over all available fields at each acquisition. Therefore, the final overall accuracy is increased by exploiting a different inversion model in each phenological stage. For this purpose, colored backgrounds represent the growth stages according to the BBCH data (as in Fig. 5). The best performance method depends not only on the date but also on the incidence angle. Hence, Table V shows the selected method at each date and incidence.

TABLE V
BEST PERFORMANCE METHOD FOR HEIGHT RETRIEVAL ALONG TIME

Incidence angle	Acquisition date (DoY)	Optimum methodology
22.7 degrees	2015.06.15 (166)	Complex coherence HH
	2015.06.26 (177)	Coherence amplitude HH
	2015.07.07 (188)	PolInSAR
	2015.07.18 (199)	Coherence amplitude HH
	2015.07.29 (210)	Complex coherence VV
	2015.08.09 (221)	Coherence amplitude HH
	2015.08.20 (232)	PolInSAR
	2015.08.31 (243)	Coherence amplitude VV
30 degrees	2015.06.17 (168)	Phase-only HH
	2015.06.28 (179)	Coherence amplitude HH
	2015.07.31 (212)	Coherence amplitude HH
	2015.08.11 (223)	Complex coherence HH
	2015.08.22 (234)	Phase-only VV
	2015.09.02 (245)	PolInSAR
39 degrees	2015.06.10 (161)	Phase-only VV
	2015.06.21 (172)	Complex coherence HH
	2015.07.02 (183)	Complex coherence VV
	2015.07.13 (194)	Complex coherence VV
	2015.07.24 (205)	Phase-only HH
	2015.08.04 (216)	Complex coherence VV
	2015.08.15 (227)	Phase-only VV
	2015.08.26 (238)	Phase-only VV

Common to all incidences, Table V corroborates that the methods which best work at the first acquisition are the ones based on the interferometric phase (i.e. phase-only or complex coherence methods). As observed in Fig. 17, these approaches avoid the overestimation due to low coherence levels at the early stages of the growth cycle. Moving forward in time, at 22.7 degrees, during the late vegetative and reproductive stages, the coherence amplitude and PolInSAR methods perform well. Nevertheless, in line with the results found in Fig. 15, the situation is different at shallower incidences. At 30 degrees, a combination of optimal methods between those based on the coherence amplitude and the complex coherence at the HH channel, which does not suffer from overestimation (as seen in Figs. 10 and 12), is observed. However, at 39 degrees, only interferometric phase-based methods are found to yield the best estimates, either exploiting the phase alone or the complex coherence. Further improvement of the final accuracy could be carried out by considering the intrinsic differences of each field.

From the final application point of view, the estimation of absolute vegetation height during the entire growth season, i.e. from a few centimeters to one meter (or more for some crops), using the same interferometric configuration (i.e., baseline) is unfeasible. The required interferometric sensitivity varies along the cultivation period, hence imposing the use of a varying observation geometry. In this sense, the usage of different methodologies as a function of the actual vegetation height, as discussed in this work, may partially solve this issue. Further experiments with different crop types are necessary to help consolidate this strategy.

ACKNOWLEDGMENT

All the TanDEM-X data were provided by the German Aerospace Center (DLR) under project NTI-POLI6736. The authors would also like to thank the support of the Federacion de Arroceros de Sevilla for providing the field data.

REFERENCES

[1] E. Erten, J. M. Lopez-Sanchez, O. Yuzugullu, and I. Hajnsek, "Retrieval of agricultural crop height from space: A comparison of SAR techniques," *Remote Sens. Environ.*, vol. 187, pp. 130–144, 2016.

[2] R. Bamler and P. Hartl, "Synthetic aperture radar interferometry," *Inverse Probl.*, vol. 14, no. 4, pp. 1–54, 1998.

[3] M. E. Engdahl, M. Borgeaud, and M. Rast, "The use of ERS-1/2 Tandem interferometric coherence in the estimation of agricultural crop heights," *IEEE Trans. Geosci. Remote Sens.*, vol. 39, pp. 1799–1806, Sept. 2001.

[4] M. Lavalle, M. Simard, and S. Hensley, "A temporal decorrelation model for polarimetric radar interferometers," *IEEE Trans. Geosci. Remote Sens.*, vol. 50, no. 7 PART 2, pp. 2880–2888, 2012.

[5] S. K. Lee, F. Kugler, K. P. Papathanassiou, and I. Hajnsek, "Quantification of temporal decorrelation effects at L-band for polarimetric SAR interferometry applications," *IEEE J. Sel. Top. Appl. Earth Obs. Remote Sens.*, vol. 6, no. 3, pp. 1351–1367, 2013.

[6] G. Krieger, A. Moreira, H. Fiedler, I. Hajnsek, M. Werner, M. Younis, and M. Zink, "TanDEM-X: A Satellite Formation for High-Resolution SAR Interferometry," *IEEE Trans. Geosci. Remote Sens.*, vol. 45, pp. 3317–3341, Nov. 2007.

[7] J. M. Lopez-Sanchez and J. D. Ballester-Berman, "Potentials of polarimetric SAR interferometry for agriculture monitoring," *Radio Sci.*, vol. 44, no. 2, 2009.

[8] C. Rossi and E. Erten, "Paddy-rice monitoring using TanDEM-X," *IEEE Trans. Geosci. Remote Sens.*, vol. 53, pp. 900–910, Feb. 2015.

[9] J. M. Lopez-Sanchez, F. Vicente-Guijalba, E. Erten, M. Campos-Taberner, and F. J. Garcia-Haro, "Retrieval of vegetation height in rice fields using polarimetric SAR interferometry with TanDEM-X data," *Remote Sens. Environ.*, vol. 192, pp. 30–44, 2017.

[10] M. Pichierri and I. Hajnsek, "Comparing Performances of Crop Height Inversion Schemes from Multifrequency Pol-InSAR Data," *IEEE J. Sel. Top. Appl. Earth Obs. Remote Sens.*, vol. 10, no. 5, pp. 1727–1741, 2017.

[11] O. Yuzugullu, E. Erten, and I. Hajnsek, "Assessment of Paddy Rice Height: Sequential Inversion of Coherent and Incoherent Models," *IEEE J. Sel. Top. Appl. Earth Obs. Remote Sens.*, vol. 11, no. 9, pp. 3001–3013, 2018.

[12] S. K. Lee, S. Y. Yoon, and J. S. Won, "Vegetation Height Estimate in Rice Fields Using Single Polarization TanDEM-X Science Phase Data," *Remote Sens.*, vol. 10, no. 11, p. 1702, 2018.

This article has been accepted for publication in a future issue of this journal, but has not been fully edited. Content may change prior to final publication. Citation information: DOI 10.1109/JSTARS.2021.3100874, IEEE Journal of Selected Topics in Applied Earth Observations and Remote Sensing

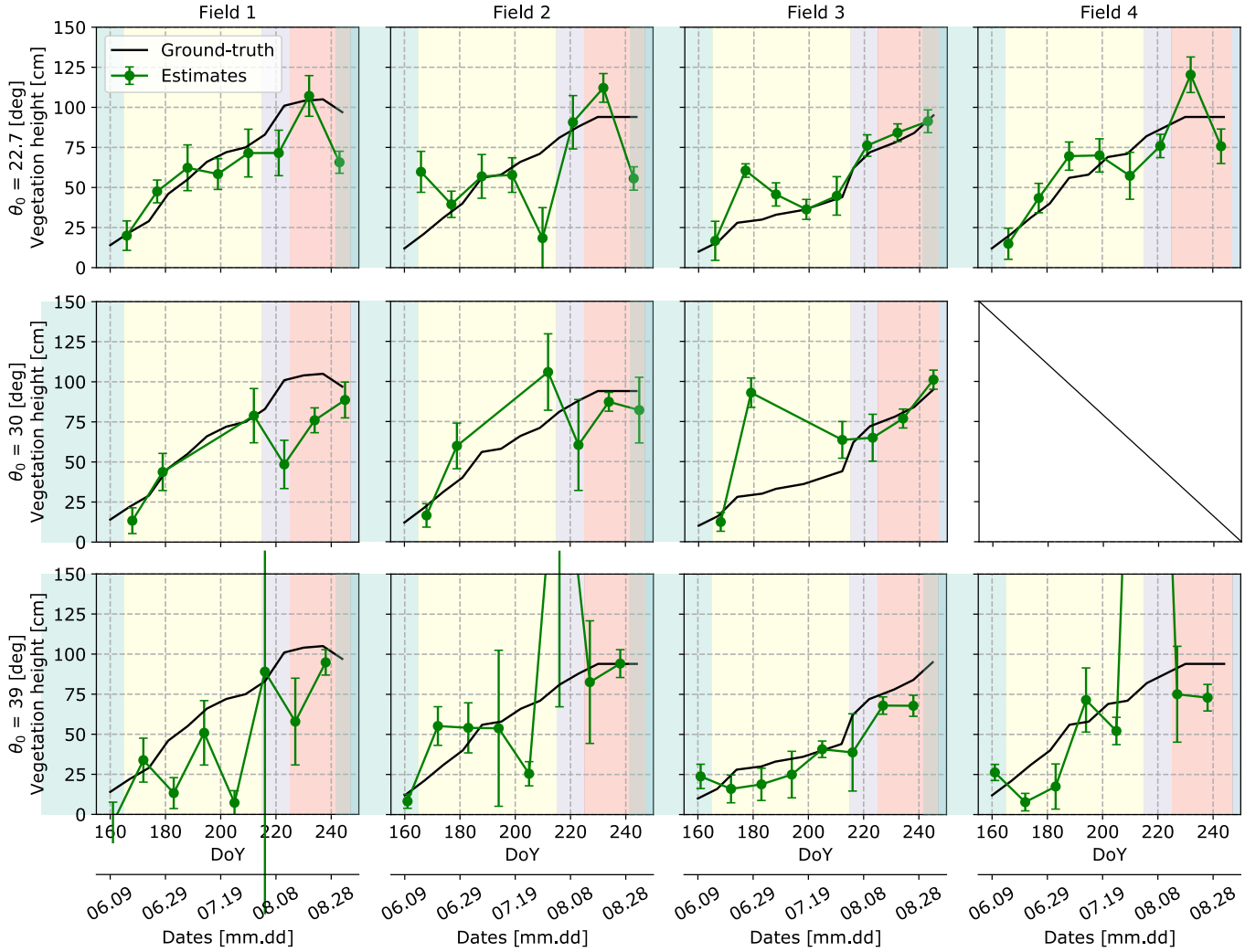

Fig. 17. Temporal evolution of the vegetation height estimates (green) and ground-truth data (black) for the monitored fields in Sevilla. Estimates are obtained from the method which shows the best performance at each acquisition. Average values are presented, and error bars denote ±one standard deviation. Colored backgrounds correspond, in average, to a different growing stage according to the BBCH scale: early and late vegetative, early and late reproductive, and maturative stages.

[13] A. Olesk, K. Voormansik, A. Vain, M. Noorma, and J. Praks, "Seasonal differences in forest height estimation from interferometric TanDEM-X coherence data," *IEEE J. Sel. Top. Appl. Earth Obs. Remote Sens.*, vol. 8, no. 12, pp. 5565–5572, 2015.

[14] A. Olesk, J. Praks, O. Antropov, K. Zalite, T. Arumae, and K. Voormansik, "Interferometric SAR coherence models for characterization of hemiboreal forests using TanDEM-X data," *Remote Sensing*, vol. 8, no. 9, p. 700, 2016.

[15] H. Chen, S. R. Cloude, and D. G. Goodenough, "Forest Canopy Height Estimation Using Tandem-X Coherence Data," *IEEE J. Sel. Top. Appl. Earth Obs. Remote Sens.*, vol. 9, pp. 3177–3188, July 2016.

[16] H. Chen, S. R. Cloude, D. G. Goodenough, D. A. Hill, and A. Nesdoly, "Radar forest height estimation in mountainous terrain using Tandem-X coherence data," *IEEE J. Sel. Top. Appl. Earth Obs. Remote Sens.*, vol. 11, pp. 3443–3452, Oct. 2018.

[17] E. Erten, C. Rossi, and O. Yüzügüllü, "Polarization Impact in TanDEM-X Data over Vertical-Oriented Vegetation: The Paddy-Rice Case Study," *IEEE Geosci. Remote Sens. Lett.*, vol. 12, pp. 1501–1505, July 2015.

[18] Junta de Andalucia, "Variedades de arroz en las marismas del Guadalquivir," 2019. Accessed on: Mar. 25, 2021. [Online]. Available: http://www.juntadeandalucia.es/.

[19] P. D. Lancashire, H. Bleiholder, T. V. D. Boom, P. Langelüddeke, R. Stauss, E. Weber, and A. Witzenberger, "A uniform decimal code for growth stages of crops and weeds," *Annals of Applied Biology*, vol. 119, no. 3, pp. 561–601, 1991.

[20] N. Romero-Puig, J. M. Lopez-Sanchez, and J. D. Ballester-Berman, "Estimation of RVoG Scene Parameters by Means of PolInSAR with TanDEM-X Data: Effect of the Double-Bounce Contribution," *IEEE Trans. Geosci. Remote Sens.*, vol. 58, pp. 7283–7304, Oct. 2020.

[21] O. Yüzügüllü, E. Erten, and I. Hajnsek, "Rice Growth Monitoring by Means of X-Band Co-polar SAR: Feature Clustering and BBCH Scale," *IEEE Geosci. Remote Sens. Lett.*, vol. 12, no. 6, pp. 1218–1222, 2015.

[22] C. Kucuk, G. Taskin, and E. Erten, "Paddy-Rice Phenology Classification Based on Machine-Learning Methods Using Multitemporal Co-Polar X-Band SAR Images," *IEEE J. Sel. Top. Appl. Earth Obs. Remote Sens.*, vol. 9, pp. 2509–2519, June 2016.

[23] J. M. Lopez-Sanchez, F. Vicente-Guijalba, J. D. Ballester-Berman, and S. R. Cloude, "Influence of incidence angle on the coherent copolar polarimetric response of rice at X-Band," *IEEE Geosci. Remote Sens. Lett.*, vol. 12, pp. 249–253, Feb. 2015.

[24] J. M. Lopez-Sanchez, F. Vicente-Guijalba, J. D. Ballester-Berman, and S. R. Cloude, "Polarimetric response of rice fields at C-band: Analysis and phenology retrieval," *IEEE Trans. Geosci. Remote Sens.*, vol. 52, pp. 2977–2993, May 2014.

[25] R. N. Treuhaft, S. N. Madsen, M. Moghaddam, and J. J. Van Zyl, "Vegetation characteristics and underlying topography from interferometric radar," *Radio Sci.*, vol. 31, pp. 1449–1485, Nov. 1996.

[26] R. N. Treuhaft and P. R. Siqueira, "Vertical structure of vegetated land surfaces from interferometric and polarimetric radar," *Radio Sci.*, vol. 35, pp. 141–177, Jan. 2000.

[27] F. Kugler, D. Schulze, I. Hajnsek, H. Pretzsch, and K. P. Papathanassiou, "TanDEM-X Pol-InSAR performance for forest height estimation," *IEEE Trans. Geosci. Remote Sens.*, vol. 52, no. 10, pp. 6404–6422, 2014.
[28] Instituto Geografico Nacional, "Centro nacional de informacion geografica," 2020. Accessed on: Mar. 25, 2021. [Online]. Available: http://www.cnig.es/home.
[29] C. Rossi, F. Rodriguez Gonzalez, T. Fritz, N. Yague-Martinez, and M. Eineder, "TanDEM-X calibrated Raw DEM generation," *ISPRS J. Photogramm. Remote Sens.*, vol. 73, pp. 12–20, Sept. 2012.
[30] R. F. Hanssen, *Radar Interferometry - Data Interpretation and Error Analysis*, vol. 2. 2001.
[31] I. Hajnsek, F. Kugler, S. K. Lee, and K. P. Papathanassiou, "Tropical-forest-parameter estimation by means of Pol-InSAR: The INDREX-II campaign," *IEEE Trans. Geosci. Remote Sens.*, vol. 47, no. 2, pp. 481–493, 2009.
[32] J. Praks, O. Antropov, and M. T. Hallikainen, "LIDAR-aided SAR interferometry studies in boreal forest: Scattering phase center and extinction coefficient at X-and L-band," *IEEE Trans. Geosci. Remote Sens.*, vol. 50, no. 10 PART1, pp. 3831–3843, 2012.
[33] M. J. Soja, H. J. Persson, and L. M. Ulander, "Estimation of forest biomass from two-level model inversion of single-pass InSAR data," *IEEE Trans. Geosci. Remote Sens.*, vol. 53, no. 9, pp. 5083–5099, 2015.
[34] S. K. Lee and T. E. Fatoyinbo, "TanDEM-X Pol-InSAR Inversion for Mangrove Canopy Height Estimation," *IEEE J. Sel. Top. Appl. Earth Obs. Remote Sens.*, vol. 8, no. 7, pp. 3608–3618, 2015.
[35] S. R. Cloude and K. P. Papathanassiou, "Single-baseline polarimetric SAR interferometry," *IEEE Trans. Geosci. Remote Sens.*, vol. 39, no. 11, pp. 2352–2363, 2001.
[36] S. R. Cloude and K. P. Papathanassiou, "Three-stage inversion process for polarimetric SAR interferometry," *IEE Proc. - Radar, Sonar Navig.*, vol. 150, no. 3, pp. 125–134, 2003.
[37] M. Martone, B. Bräutigam, and G. Krieger, "Quantization effects in TanDEM-X data," *IEEE Trans. Geosci. Remote Sens.*, vol. 53, pp. 583–597, Feb. 2015.
[38] K. Sarabandi and Y. C. Lin, "Simulation of interferometric SAR response for characterizing the scattering phase center statistics of forest canopies," *IEEE Trans. Geosci. Remote Sens.*, vol. 38, no. 1 I, pp. 115–125, 2000.
[39] E. Colin, C. Titin-Schnaider, L. Thirion, and W. Tabbara, "Comparison between simulations and interferometric polarimetric SAR P-band data on a pine-trees forest," in *Int. Geosci. Remote Sens. Symp.*, vol. 5, pp. 3128–3131, IEEE, 2004.
[40] S. R. Cloude, *Polarisation: Applications in Remote Sensing*. Oxford: Oxford University Press, 2009.
[41] M. Martone, P. Rizzoli, and G. Krieger, "Volume Decorrelation Effects in TanDEM-X Interferometric SAR Data," *IEEE Geosci. Remote Sens. Lett.*, vol. 13, pp. 1812–1816, Dec. 2016.

PLACE PHOTO HERE

Noelia Romero-Puig received the B.Sc. degree in Sound and Image in Telecommunications Engineering and the M.Sc. degree in Telecommunication Engineering from the University of Alicante, Spain, in 2016 and 2018, respectively, where she is currently pursuing the Ph.D. degree with the Signals, Systems and Telecommunication Group.

Her research interests include monitoring of agricultural crops by means of SAR interferometry (InSAR) and polarimetric SAR interferometry (PolInSAR) techniques.

Ms. Noelia Romero-Puig was a recipient of the Award for Best Final Master's Project in Remote Sensing defended in Spain in 2018 of the IEEE GRSS Spanish Chapter and the Hisdesat Award for the Best Final Master's Project in Government Satellite Services by the Official College of Telecommunications Engineers (COIT).

PLACE PHOTO HERE

Juan M. Lopez-Sanchez (S'94, M'00, SM'05) was born in Alicante, Spain, in 1972. He received the Ingeniero (M.S). and Doctor Ingeniero (Ph.D.) degrees in Telecommunication Engineering from the Technical University of Valencia (UPV), Valencia, Spain, in 1996 and 2000, respectively. From 1998 to 1999 he worked as a predoctoral grantholder at the Space Applications Institute, Joint Research Centre of the European Commission, Ispra, Italy. Since 2000 he leads the Signals, Systems and Telecommunication Group of the University of Alicante, Spain, where he is full professor since November 2011.

His main research interests include microwave remote sensing for inversion of biophysical parameters, polarimetric and interferometric techniques, and applications of radar remote sensing in agriculture and geophysics.

In 2001, Dr. Lopez-Sanchez received the Indra Award for the best Ph.D. thesis about radar in Spain. From 2006 to 2012 he was the Chair of the Spanish Chapter of the IEEE Geoscience and Remote Sensing Society. He has coauthored more than 80 papers in refereed journals and more than 130 papers and presentations in international conferences and symposia.